Structure and reaction of a deformed halo nucleus

Kouichi Hagino
(Tohoku University)

Yasuko Urata (Tohoku)
Hiroyuki Sagawa (Aizu)

TOHOKU UNIVERSITY

1. Deformed halo nucleus: what is it?
2. Single-particle motion in a deformed potential
3. Particle-rotor model and its appliation to ^{31}Ne
4. Coulomb breakup and reaction cross section
(5. Even-odd Staggering of reaction cross section)
6. Summary

What is “deformed halo”? : definition

halo nucleus: weakly bound valence particle(s) with a core nucleus

halo + core deformation:

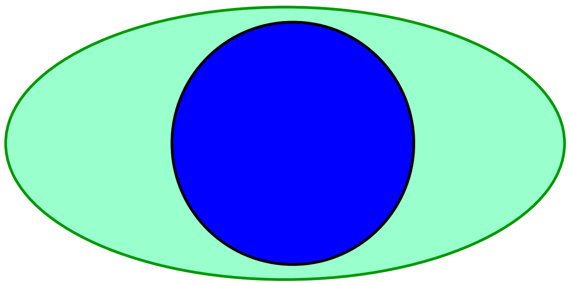

spherical core
+ deformed valence
orbit

cf. ^{17}O : slightly oblate

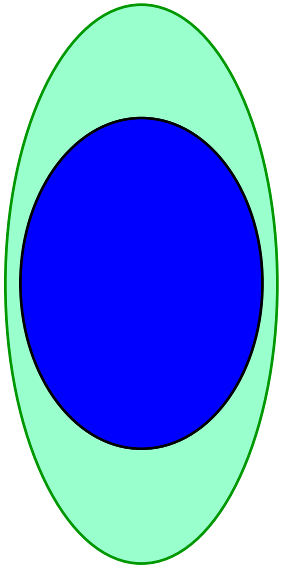

deformed core
+ def. orbit

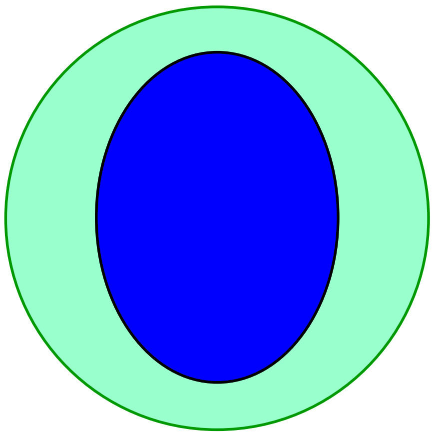

deformed core
+ spherical orbit

deformed halo nucleus

Well-known example: ^{11}Be (S$_n$ = 504 +/- 6 keV)

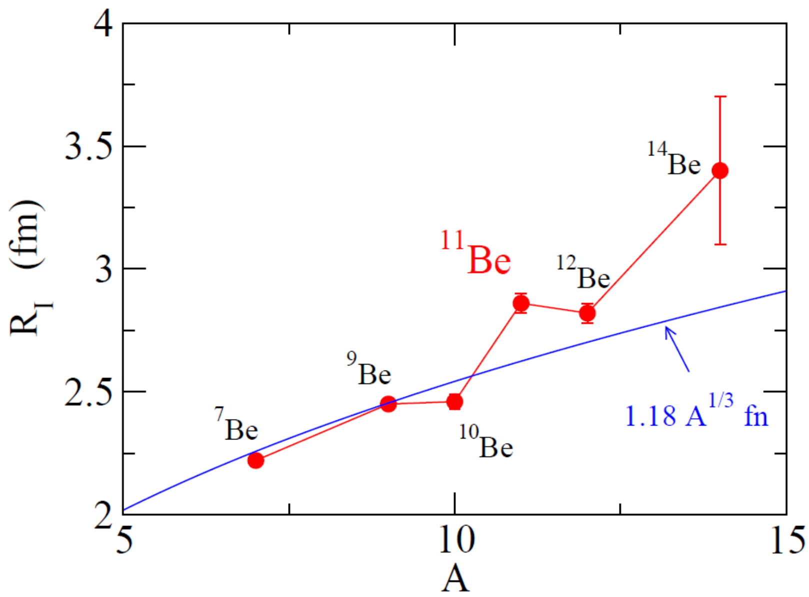

I. Tanihata et al.,
PRL55(‘85)2676; PLB206(‘88)592

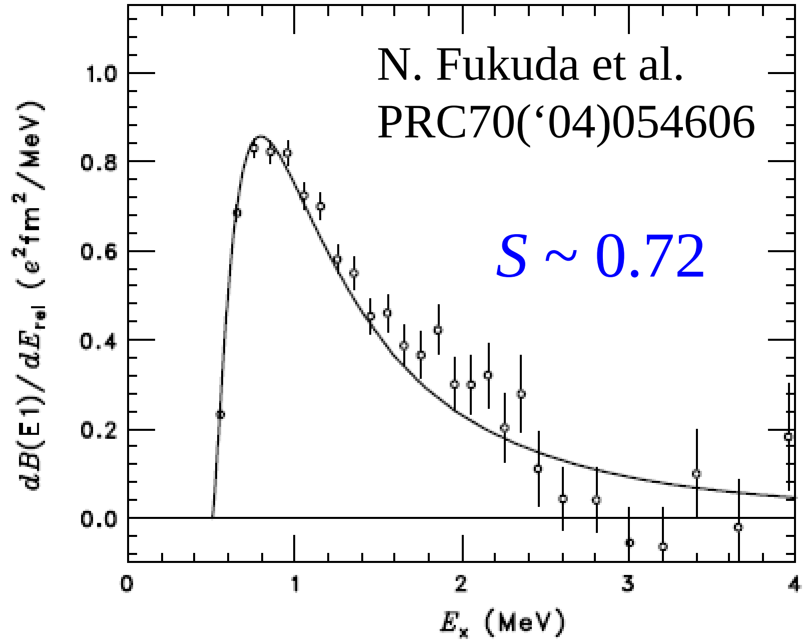

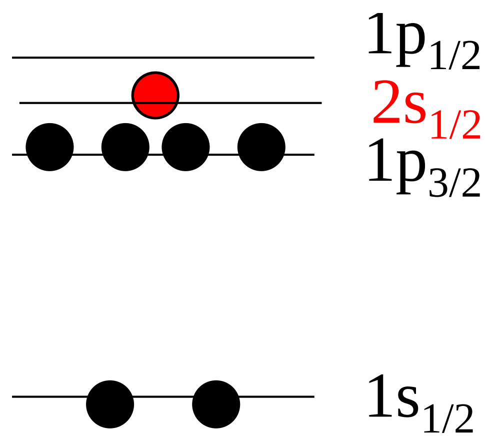

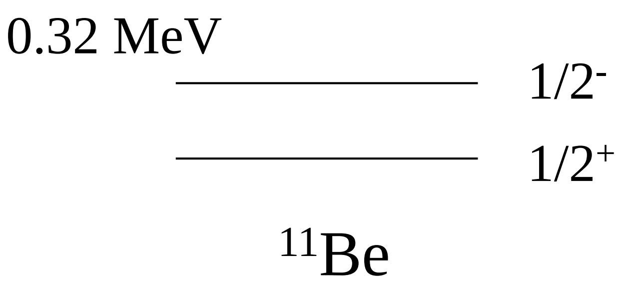

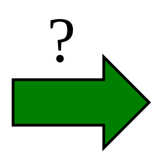

“parity inversion”

deformed ^{11}Be ? ⟶ single-particle motion in a deformed potential

Can deformation effect explain the level scheme of ^{11}Be ?

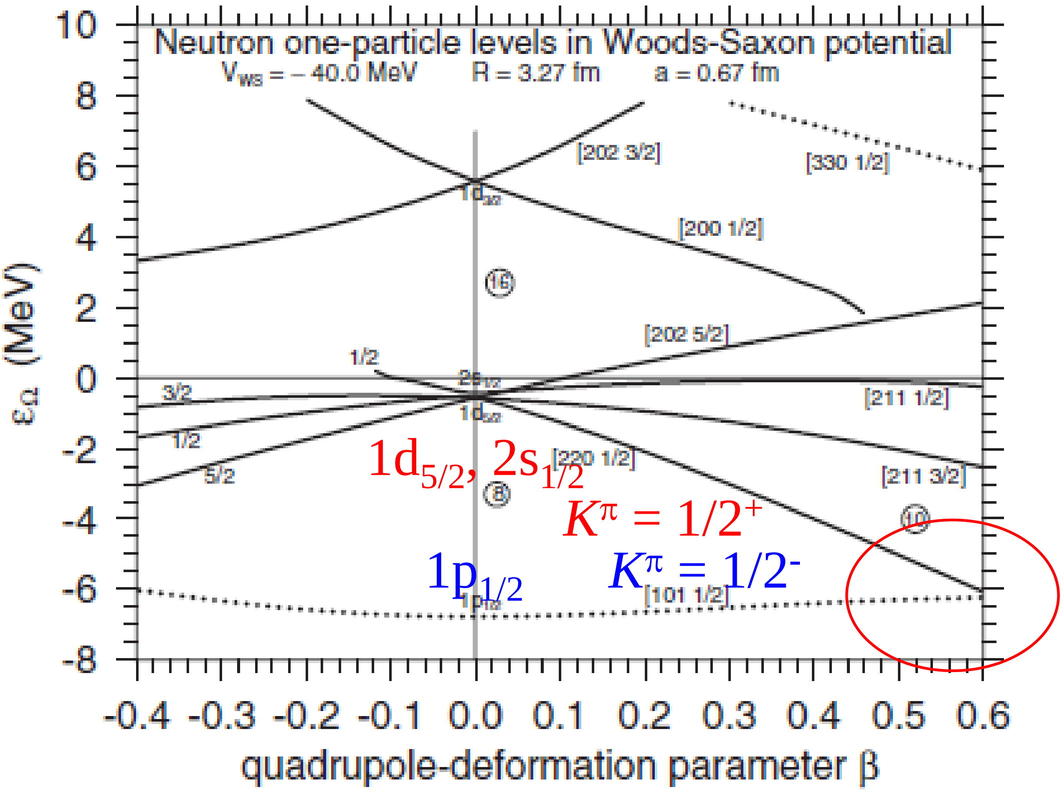

I. Hamamoto, J. Phys. G37('10)055102

s.p. motion in a deformed potential, $V(r,\theta)$

← inversion of + parity and – parity states at large deformation

cf. <u>coupled-channels calculation with finite core excitation energies</u>:

H. Esbensen, B.A. Brown, H. Sagawa, PRC51('95)1274

F.M. Nunes, I.J. Thompson, R.C. Johnson, NPA596('96)171

Role of s.p. angular momentum in halo formation

$$\langle r^2 \rangle \propto \begin{cases} 1/|\epsilon_0| & (l=0) \\ 1/\sqrt{|\epsilon_1|} & (l=1) \\ const. & (l=2) \end{cases}$$

K. Riisager, A.S. Jensen, and P. Moller, NPA548('92)393

⇓

radius: diverges for $l = 0,1$ in the zero binding limit

⇓

halo (anomalously large radius) : $l = 0$ or 1

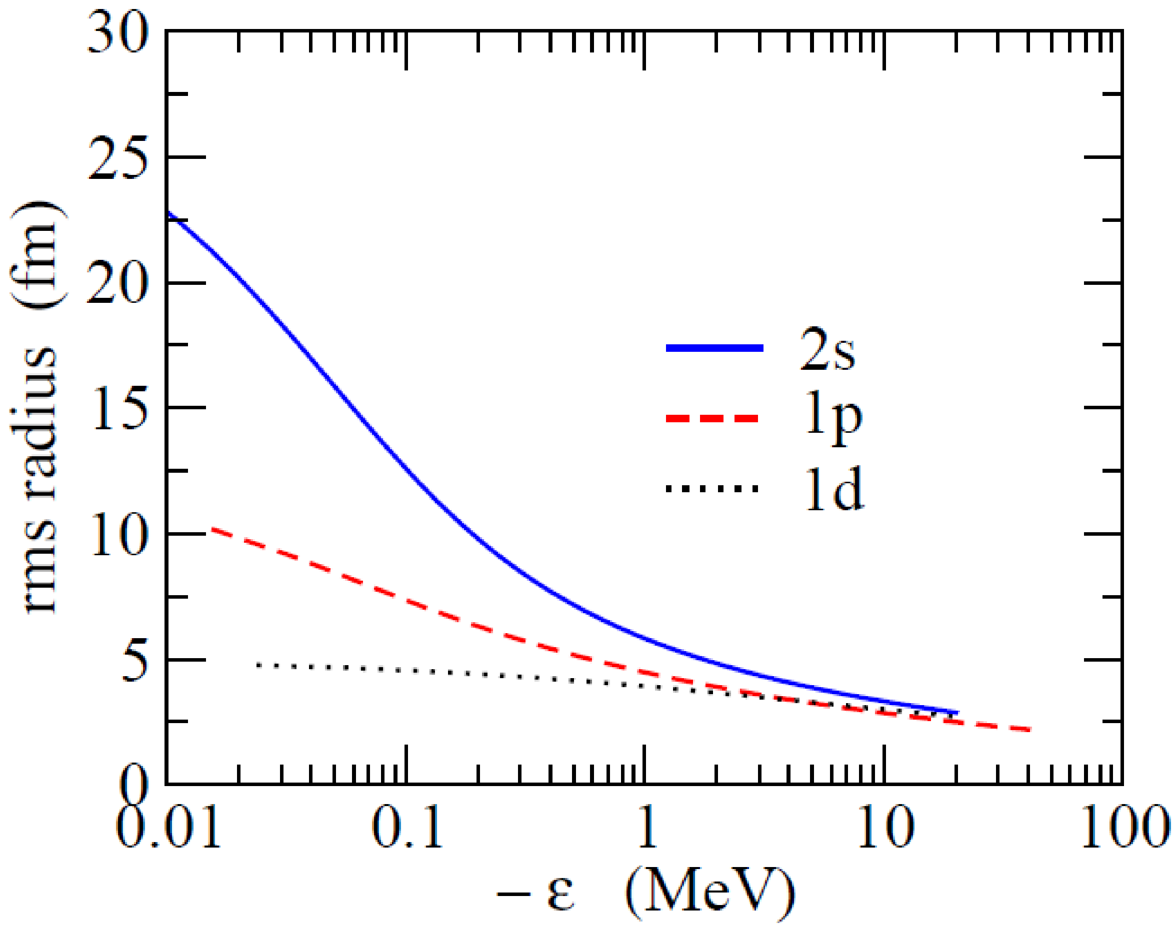

K.H., I. Tanihata, and H. Sagawa, arXiv: 1208.1583

s.p. motion in a deformed potential

halo : only for l = 0 or 1

⇨ however, a possibility is enlarged for a deformed nucleus

deformed potential $V(r,\theta)$ ⟶ mixture of angular momenta

e.g.,

$$|d_{5/2}\rangle \to |d_{5/2}\rangle + |s_{1/2}\rangle + |g_{7/2}\rangle + \cdots$$

$$|f_{7/2}\rangle \to |f_{7/2}\rangle + |p_{3/2}\rangle + |p_{1/2}\rangle + \cdots$$

(note) $s_{1/2}$: $\Omega^\pi = 1/2^+$ only
$p_{1/2}$: $\Omega^\pi = 1/2^-$ only
$p_{3/2}$: $\Omega^\pi = 3/2^-$ and $1/2^-$ only

⟶ possibility of halo only for s.p. states with $\Omega^\pi = 1/2^+, 1/2^-, 3/2^-$

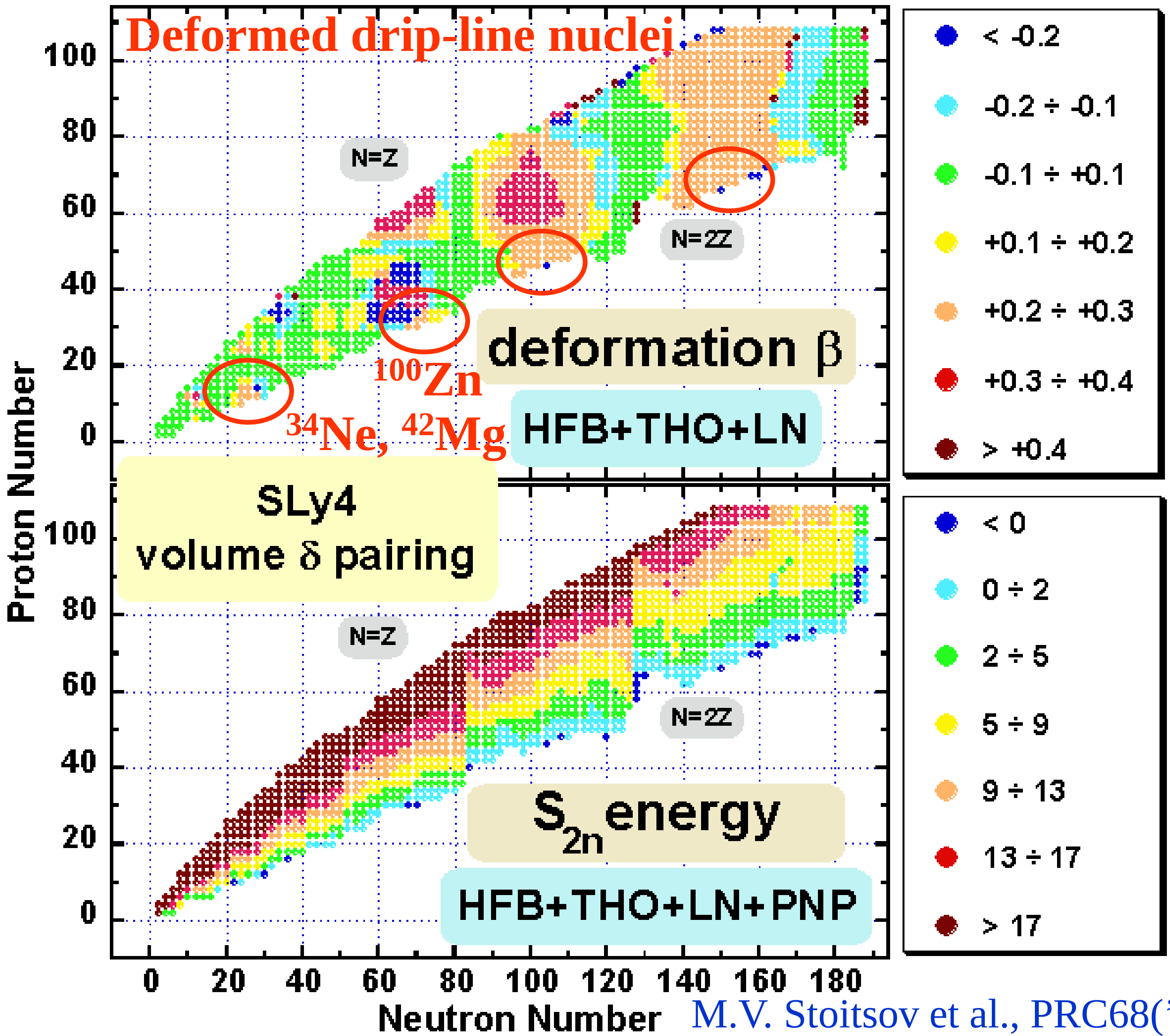

^{32}Ne:
β=0.151
^{34}Ne:
β=0.277
^{42}Mg:
β=-0.18
^{100}Zn:
β=0.244

M.V. Stoitsov et al., PRC68('03)054312

s-wave dominance phenomenon

$$|d_{5/2}\rangle \;\to\; |d_{5/2}\rangle + |s_{1/2}\rangle + |g_{7/2}\rangle + \cdots$$
$$\to\; |s_{1/2}\rangle \qquad (|\epsilon| \to 0)$$

T. Misu, W. Nazarewicz,
and S. Aberg, NPA614('97)44
(deformed square well)

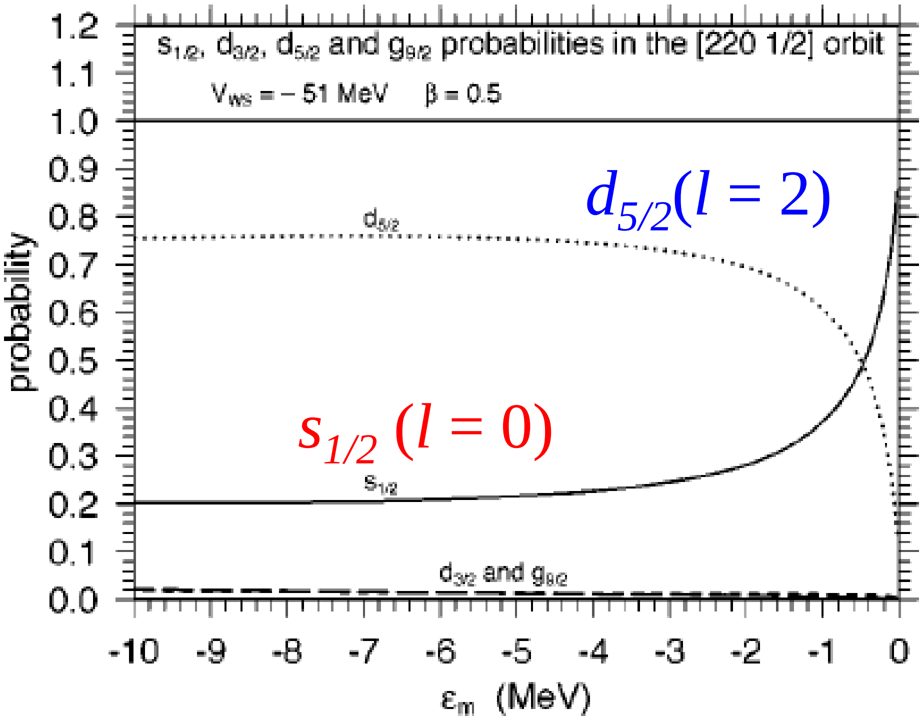

I. Hamamoto, PRC69('04)041306(R)
(deformed Woods-Saxon)

reason for *s*-wave dominance

$$\Psi_K(\boldsymbol{r}) = \sum_l R_l(r) Y_{lK}(\hat{\boldsymbol{r}}) \equiv \sum_l \psi_{lK}(\boldsymbol{r})$$

$$P_l = \frac{\langle\psi_{lK}|\psi_{lK}\rangle}{\langle\Psi|\Psi\rangle} = \frac{\langle\psi_{lK}|\psi_{lK}\rangle}{\sum_{l'}\langle\psi_{l'K}|\psi_{l'K}\rangle}$$

(note) $\langle\psi_{lK}|\psi_{lK}\rangle$ diverges for $l = 0$ ($\varepsilon \to 0$)
finite for $l > 0$

$$P_l \sim \frac{\langle\psi_{lK}|\psi_{lK}\rangle}{\langle\psi_{0K}|\psi_{0K}\rangle} = 1 \quad (l = 0)$$

(note)

$$\beta_2 \propto \frac{\langle r^2 Y_{20}\rangle}{\langle r^2\rangle} \to 0 \quad (\epsilon \to 0)$$

similar dominance phenomenon for *p*-wave

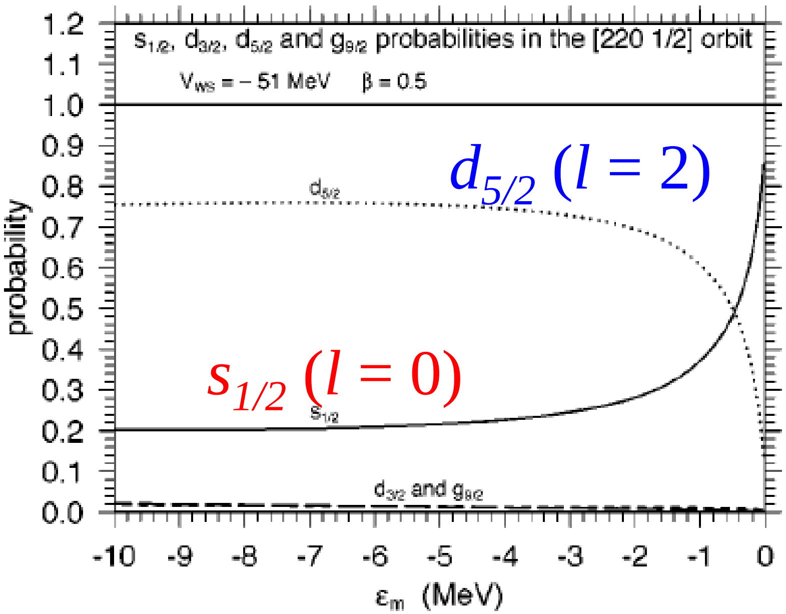

I. Hamamoto, PRC69(‘04)041306(R)

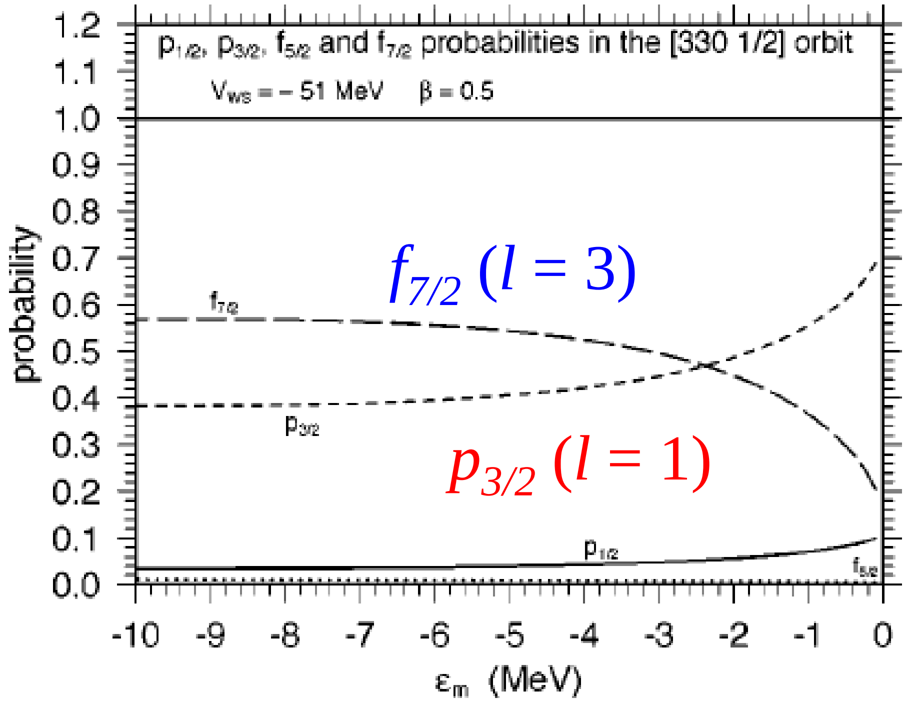

(enhancement of p-wave component, although not 100% in the zero binding limit)

c.f. s-wave dominance and s.p. resonance:
K. Yoshida and K.H., PRC72(‘05) 064311

c.f. s-wave dominance and s.p. resonance:

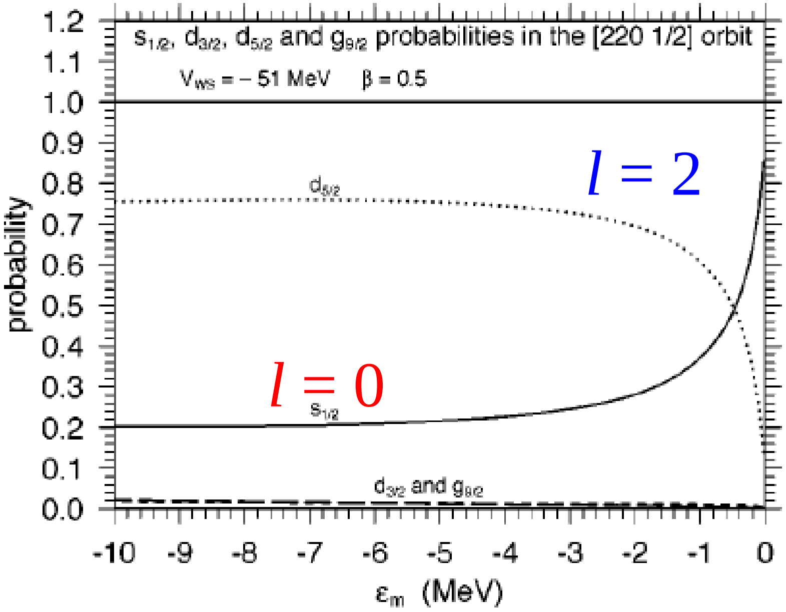

I. Hamamoto, PRC69('04)041306(R)

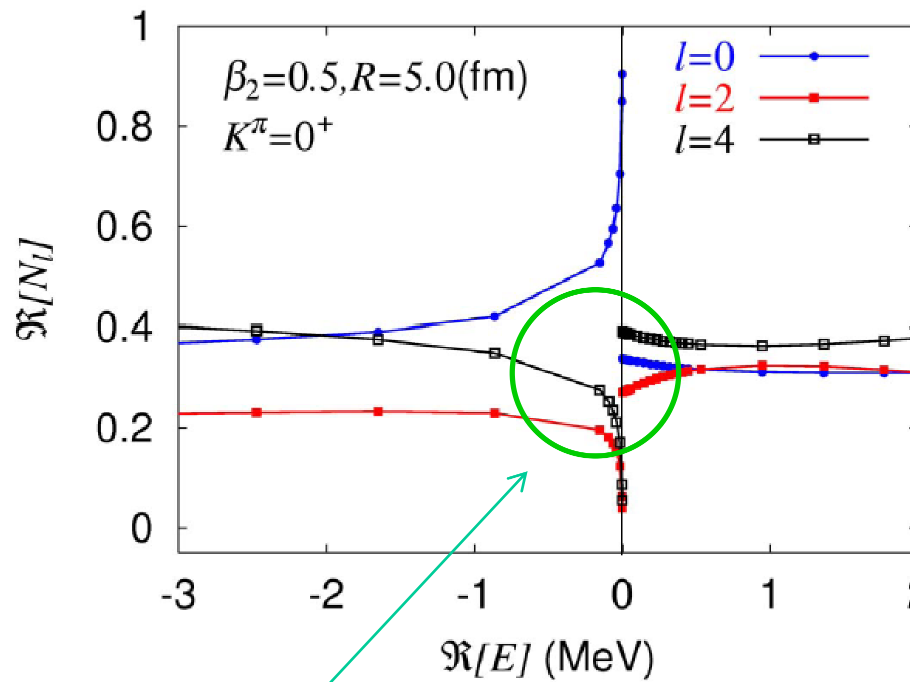

The s-wave dominance phenomenon does not continue to scattering states → existence of a $K^\pi = 0^+$ resonance

K. Yoshida and K. Hagino, PRC72('05)064311

particle-rotor model

Nilsson model: intrinsic (body-fixed) frame formalism
(mixing of angular momenta)

⟶ transformation to the lab. frame

✓angular momentum projection
✓particle-rotor model

core + neutron two-body model
with core excitations

$$\Psi_{IM} = \sum_{I_c,j,l} \left(\quad \right)^{(IM)}$$

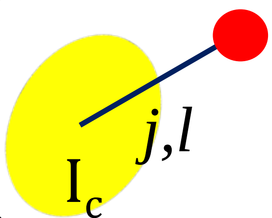

$$= |0^+ \otimes p_{3/2}\rangle + |2^+ \otimes f_{7/2}\rangle + \cdots$$

e.g.,

For an axially symmetric rotor,
Nilsson: adiabatic (strong coupling) limit of particle-rotor model

particle-rotor model

particle-rotor model:

coupling between particle and rotor

$$H = -\frac{\hbar^2}{2m}\nabla^2 + V_0(r_n) + V_{\rm def}(r_n, \hat{\boldsymbol{r}}_c, \hat{\boldsymbol{r}}_n) + H_{\rm rot}$$

$$\Psi_{IM} = \sum_{I_c,j,l} \Big[\quad \Big]^{(IM)} = \sum_{I_c,j,l} R^{(I)}_{I_cjl}(r_n)|[(jl)I_c]^{(IM)}\rangle$$

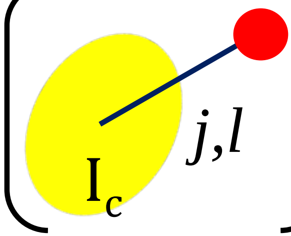

coupled-channels equations

non-adiabatic effect

$$\left(-\frac{\hbar^2}{2m}\frac{d^2}{dr^2} + \frac{l(l+1)\hbar^2}{2mr^2} + V_0(r) + E_{I_c} - \epsilon\right) R^{(I)}_{I_cjl}(r)$$

$$= -\sum_{I'_c,j',l'} \langle [(jl)I_c]^{(IM)}|V_{\rm def}|[(j'l')I'_c]^{(IM)}\rangle R^{(I)}_{I'_cj'l'}(r)$$

adiabatic limit of particle-rotor model

Nilsson: adiabatic (strong coupling) limit of particle-rotor model

$$H = -\frac{\hbar^2}{2m}\nabla^2 + V(r_n, \hat{\boldsymbol{r}}_c, \hat{\boldsymbol{r}}_n) + H_{\rm rot}$$

$H_{\rm rot} \rightarrow$ 0 (degenerate rotational band)

$\longrightarrow$ K : a good quantum number (no Coriolis coupling)

body fixed frame

$$h = -\frac{\hbar^2}{2m}\nabla^2 + V(r_n, \theta_{cn})$$

$$\Psi_{IM} \rightarrow \Phi_K = \sum_{j,l} \phi_{jlK}(r_n)|jlK\rangle$$

$$R^{(I)}_{I_cjl}(r) = A^{IK}_{jI_c} \cdot \phi_{jlK}(r)$$

particle-rotor Nilsson

$$A^{IK}_{jI_c} = \sqrt{\frac{2I_c+1}{2I+1}} \cdot \sqrt{2}\,\langle jKI_c0|IK\rangle$$

H. Esbensen and C.N. Davids, PRC63('00)014315

particle-rotor model with finite excitation energy

coupled-channels equations

non-adiabatic effect

$$\left(-\frac{\hbar^2}{2m}\frac{d^2}{dr^2}+\frac{l(l+1)\hbar^2}{2mr^2}+V_0(r)+E_{I_c}-\epsilon\right)R^{(I)}_{I_cjl}(r)$$
$$=-\sum_{I'_c,j',l'}\langle[(jl)I_c]^{(IM)}|V_{\rm def}|[(j'l')I'_c]^{(IM)}\rangle R^{(I)}_{I'_cj'l'}(r)$$

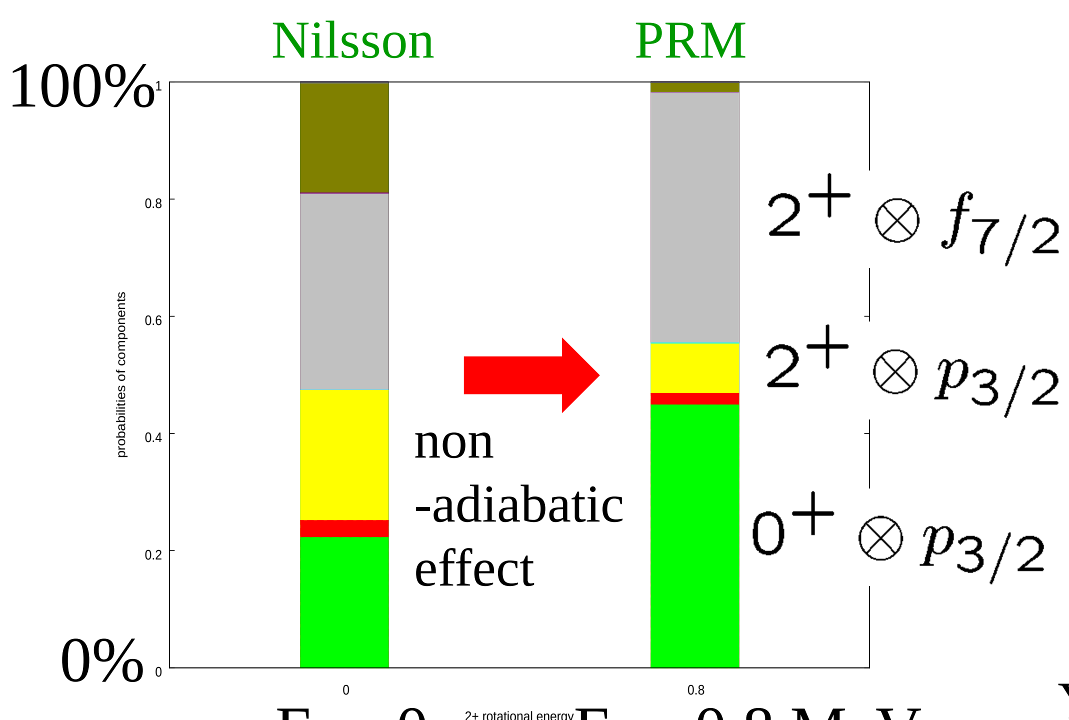

E_{2+}=0 E_{2+}=0.8 MeV

example:

[330 1/2] level at β=0.2

↑

21st neutron

ε = -0.3 MeV

spherical basis with R_{box}=60 fm

Y. Urata, K.H., and H. Sagawa, PRC83(‘11)041303(R)

Application to ^{31}Ne

large Coulomb breakup and interaction cross sections

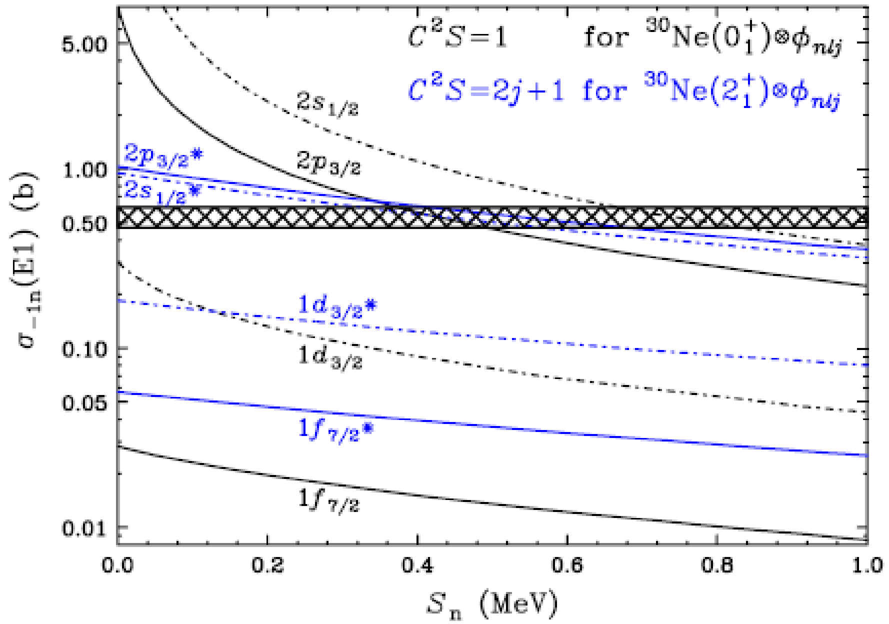

T. Nakamura et al., PRL103(‘09)262501

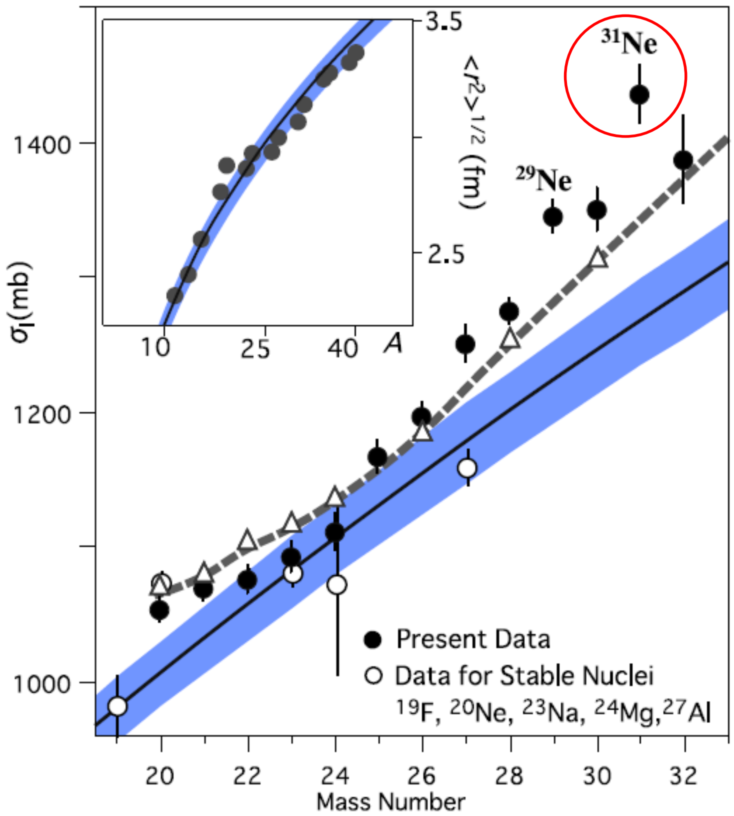

M.Takechi et al., PLB 707(‘12)357

theoretical studies:

- W. Horiuchi et al., PRC81(‘10)024606
- I. Hamamoto, PRC81(‘10)021304(R)
- Y. Urata, K.H., H. Sagawa, PRC83(‘11)041303(R); PRC86(‘12)044613
- K. Minomo et al., PRL108(‘12)052503; PRC84(‘11)034602; PRC85(‘12)064613

Nilsson model analysis [I. Hamamoto, PRC81('10)021304(R)]

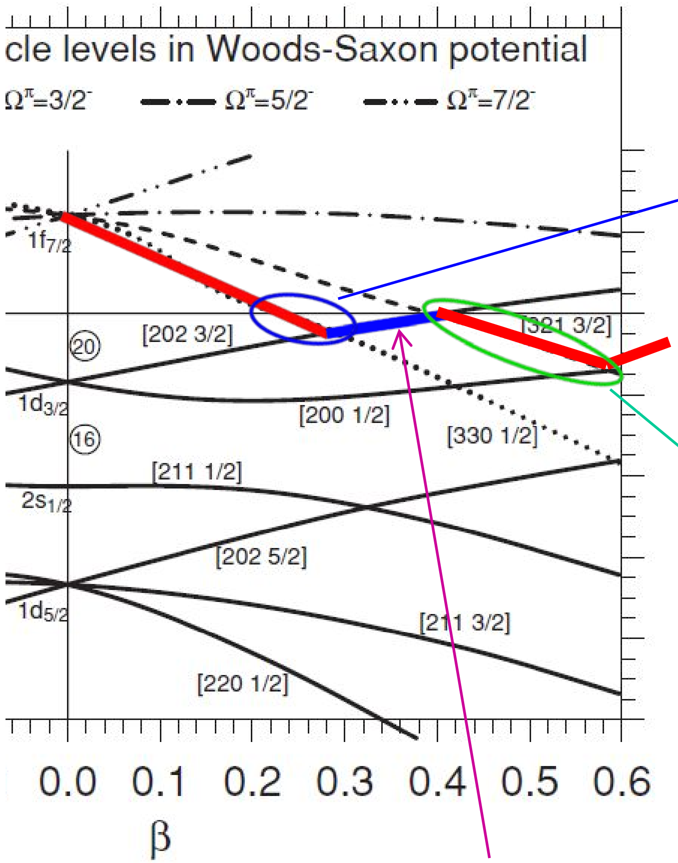

21st neutron

non-halo

$(\Omega^\pi = 3/2^+)$

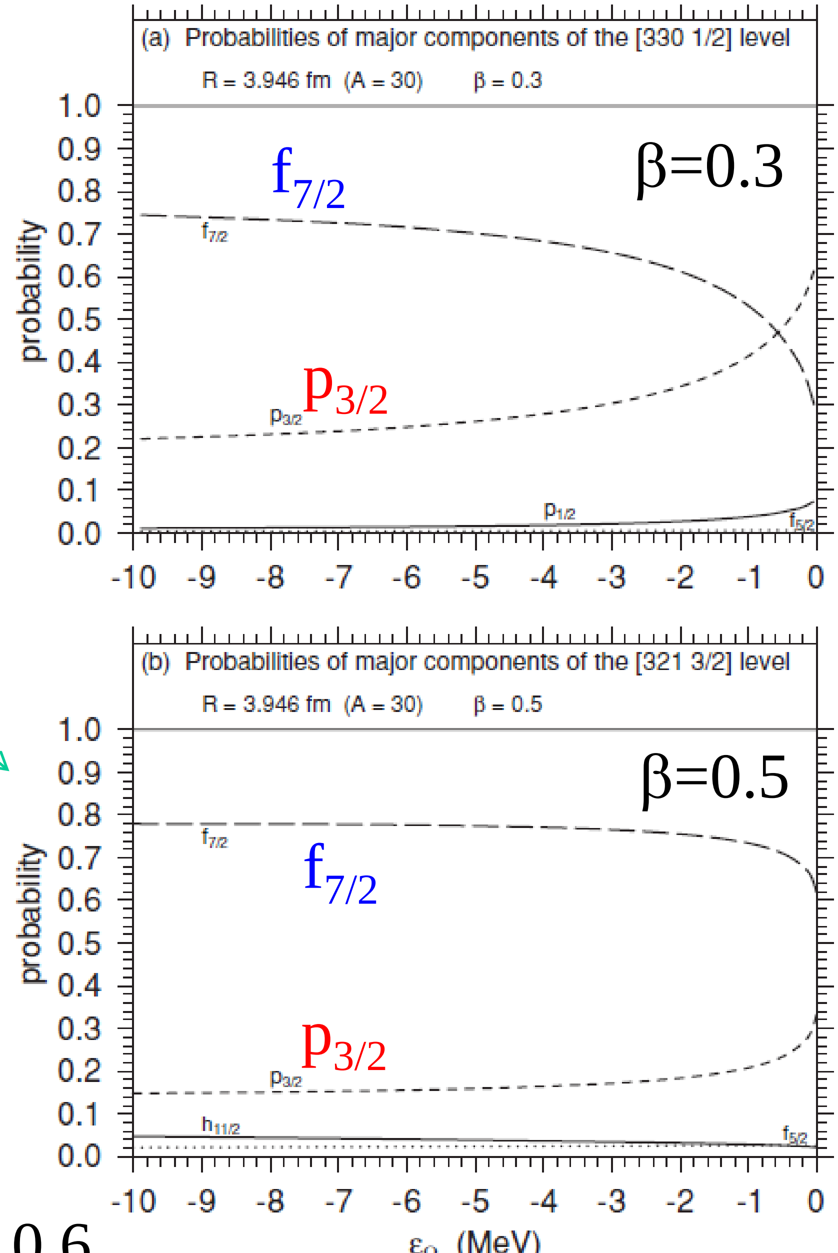

* also [200 1/2+] if S_n > 500 keV, β > 0.6

Nilsson model analysis [I. Hamamoto, PRC81('10)021304(R)]

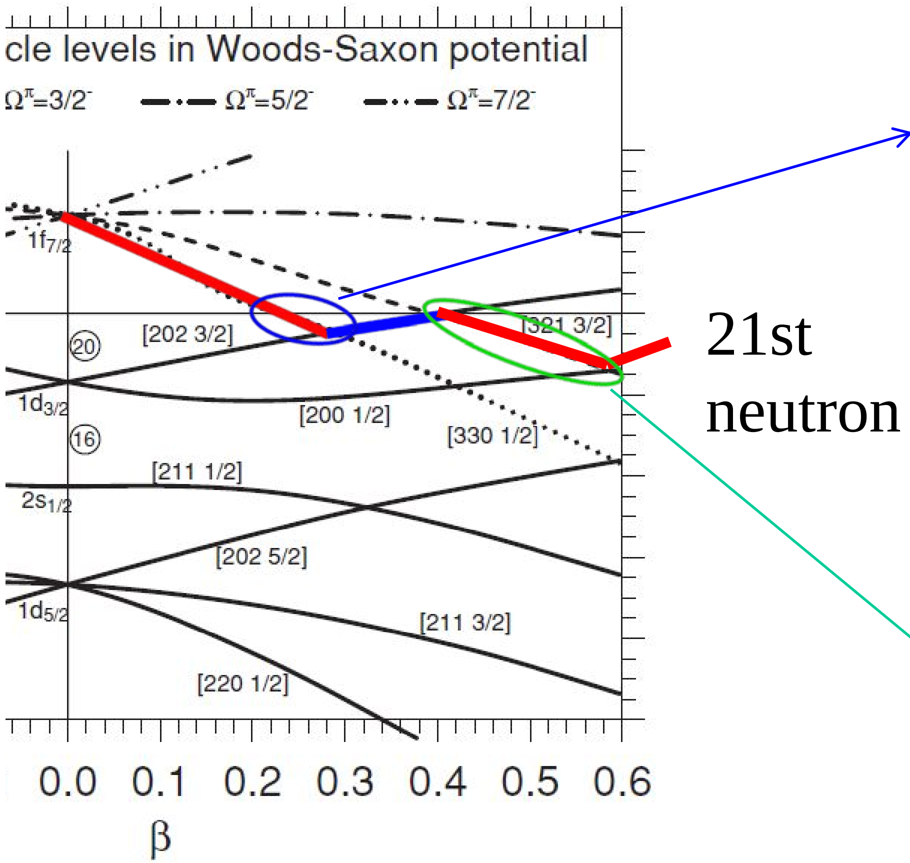

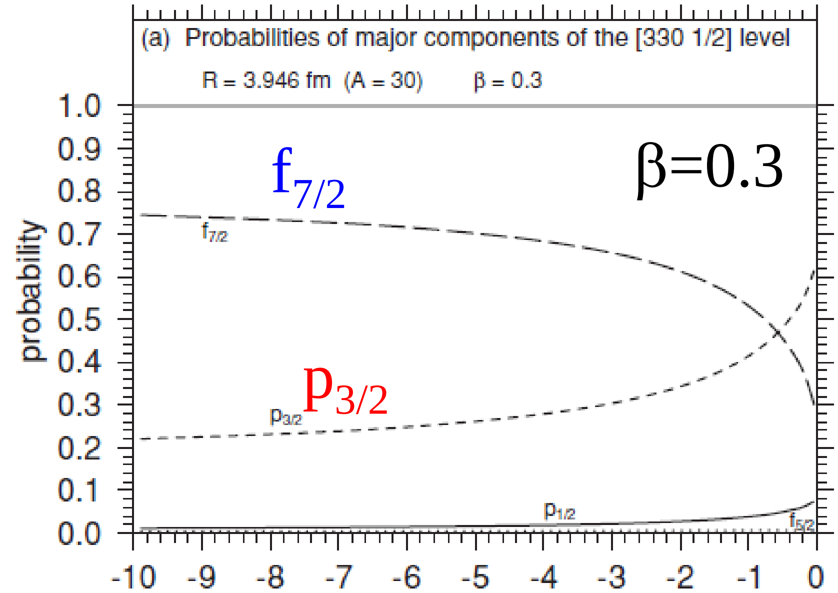

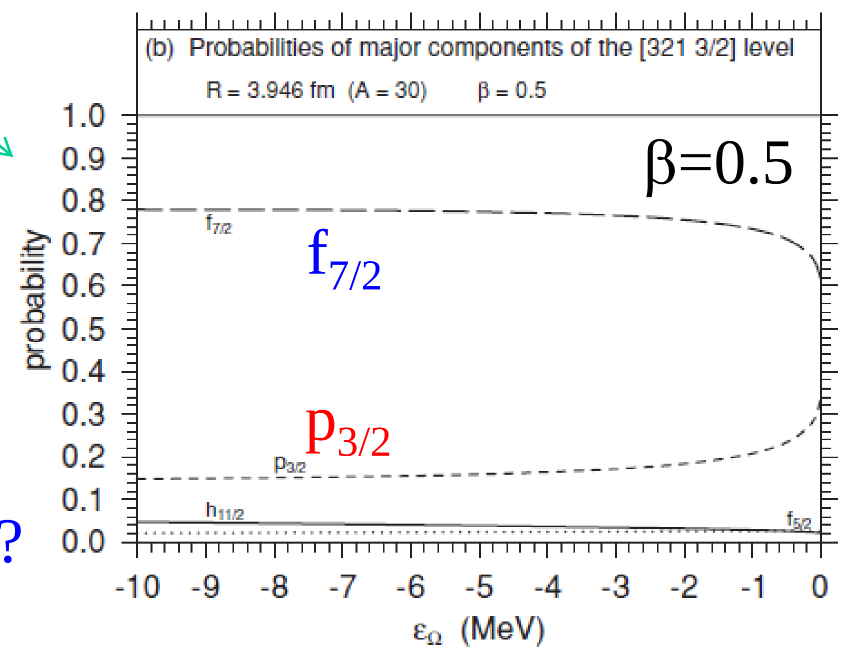

- non-adiabatic effects?
- comparison to the data (σ_{bu} and σ_I)?

Coulomb breakup

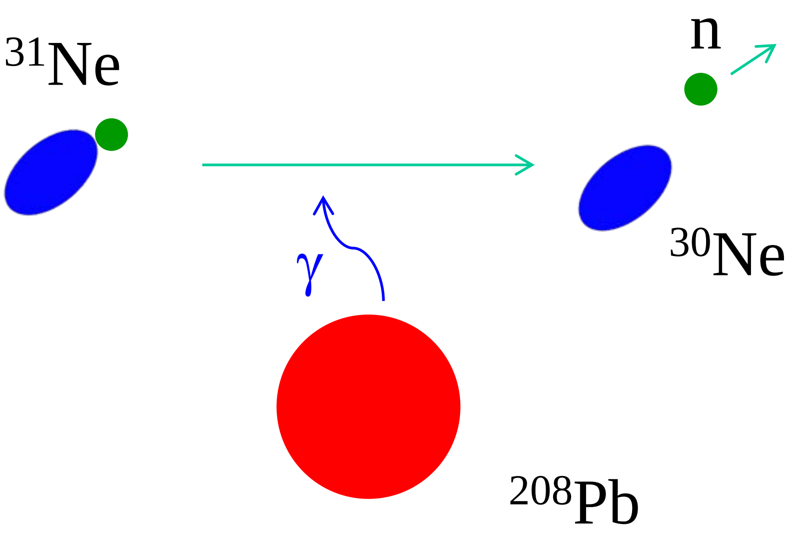

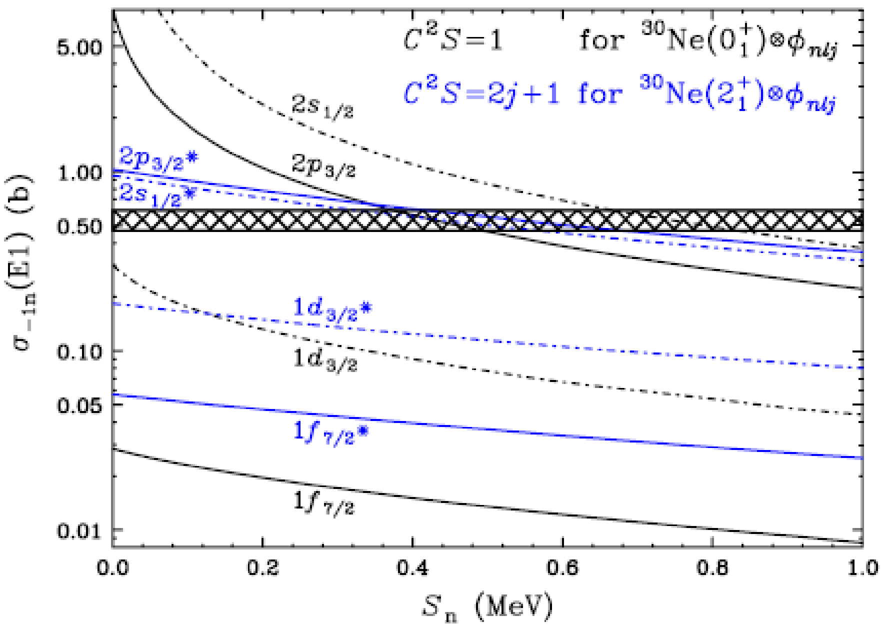

T. Nakamura et al., PRL103('09)262501

1st order perturbation theory

$$\sigma = \sum_f \frac{16\pi^3}{9\hbar c} \cdot N_{\mathrm{E1}}(E_f - E_i) \cdot B(E1; i \to f)$$

$$B(E1; i \to f) = \frac{1}{2I_i + 1} \left| \left\langle \Psi_f \left\| \hat{D} \right\| \Psi_i \right\rangle \right|^2$$

$$\hat{D}_\mu = -[Z_c e/(A_c + 1)] \cdot rY_{1\mu}(\hat{\boldsymbol{r}})$$

Coulomb breakup cross sections

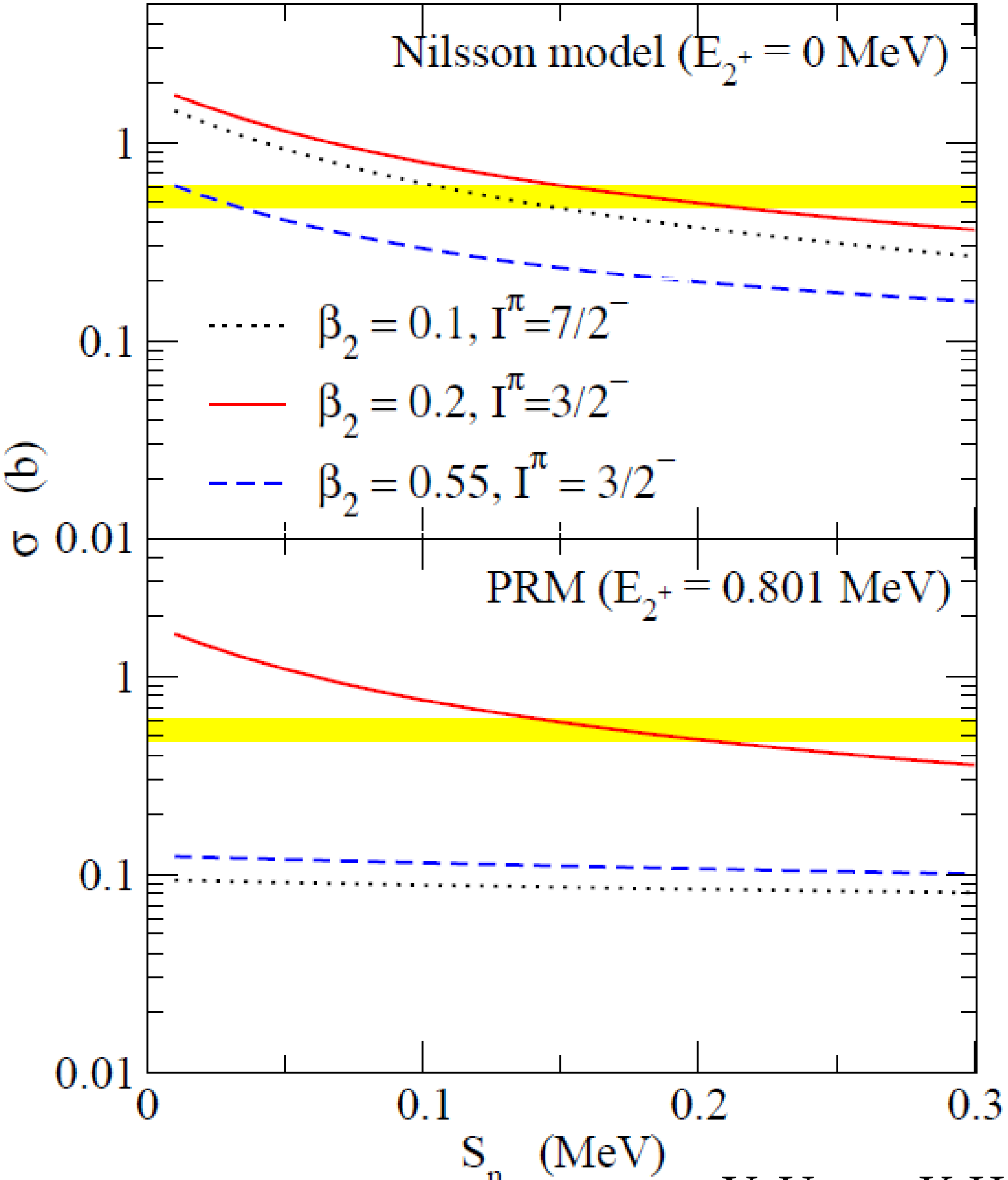

E_{2+} (^{30}Ne) = 0.801(7) MeV
P. Doornenbal et al., PRL103('09)032501

S_n (^{31}Ne) = 0.29 +/- 1.64 MeV

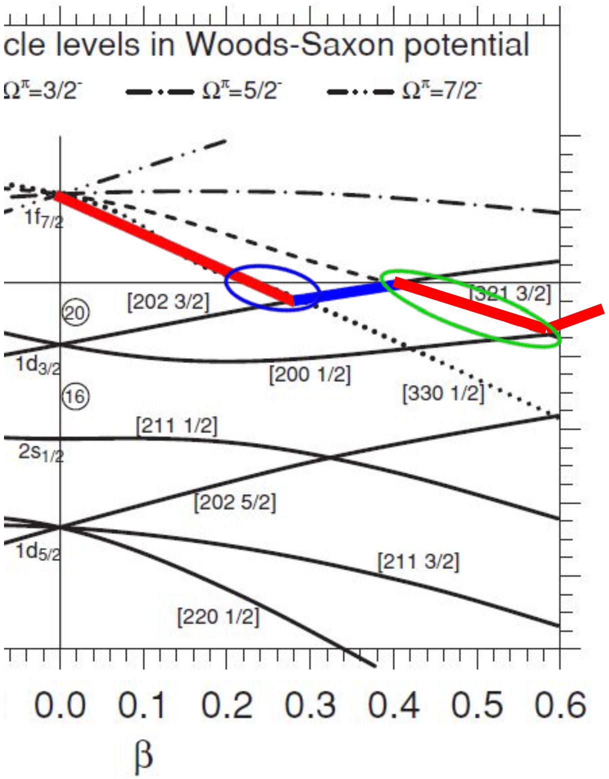

Y. Urata, K.H., and H. Sagawa, PRC83('11)041303(R)

Coulomb breakup cross sections (β ~ 0.2 configuration)

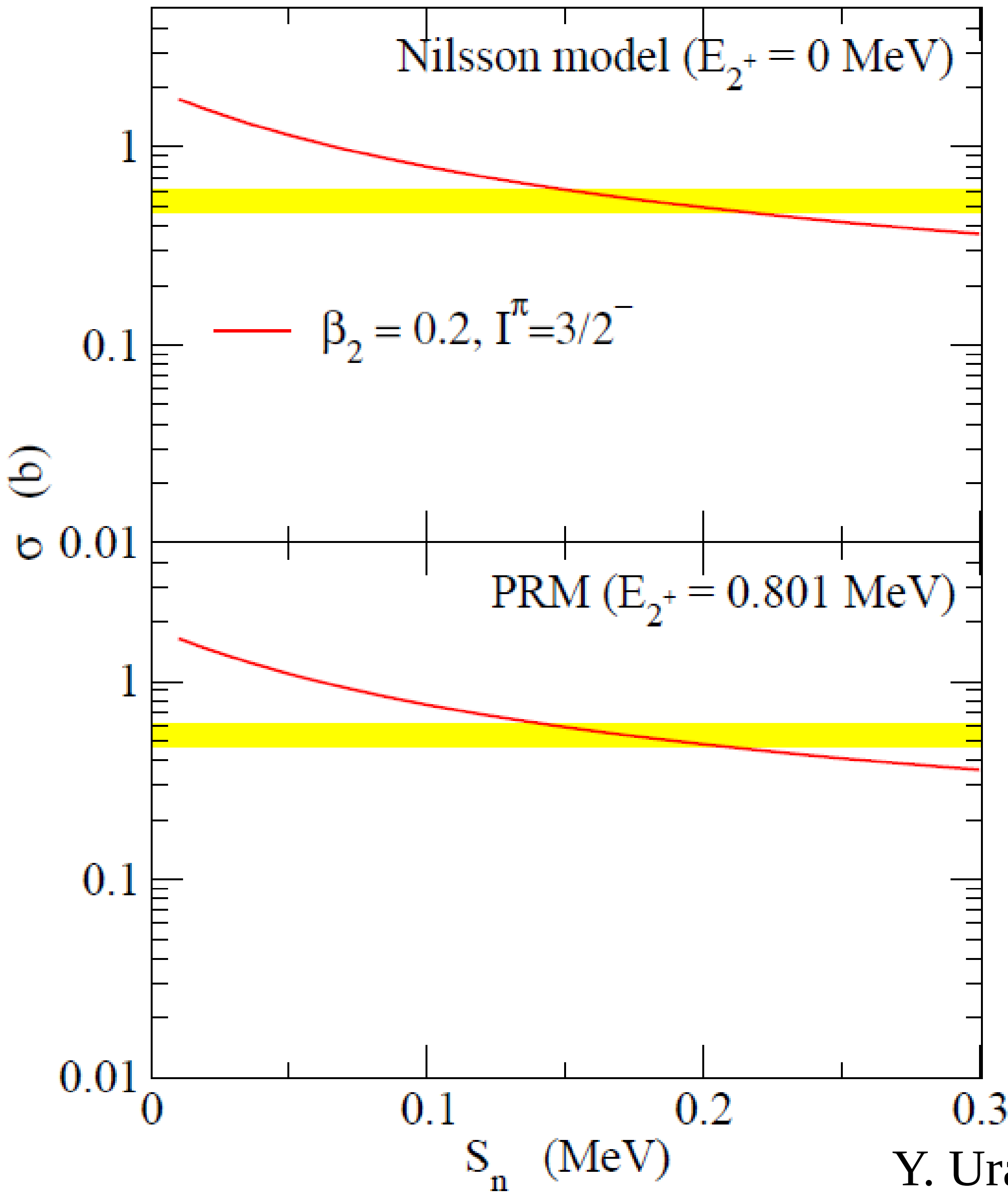

β ~ 0.2 : small non-adiabatic effects

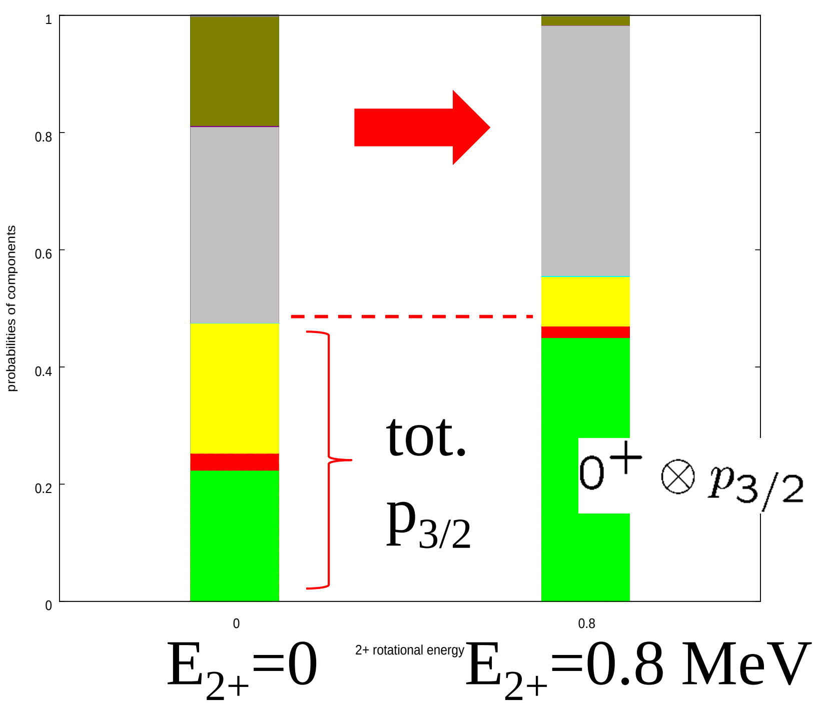

Y. Urata, K.H., and H. Sagawa, PRC83('11)041303(R)

Coul. b.u. with final 0^+ core state

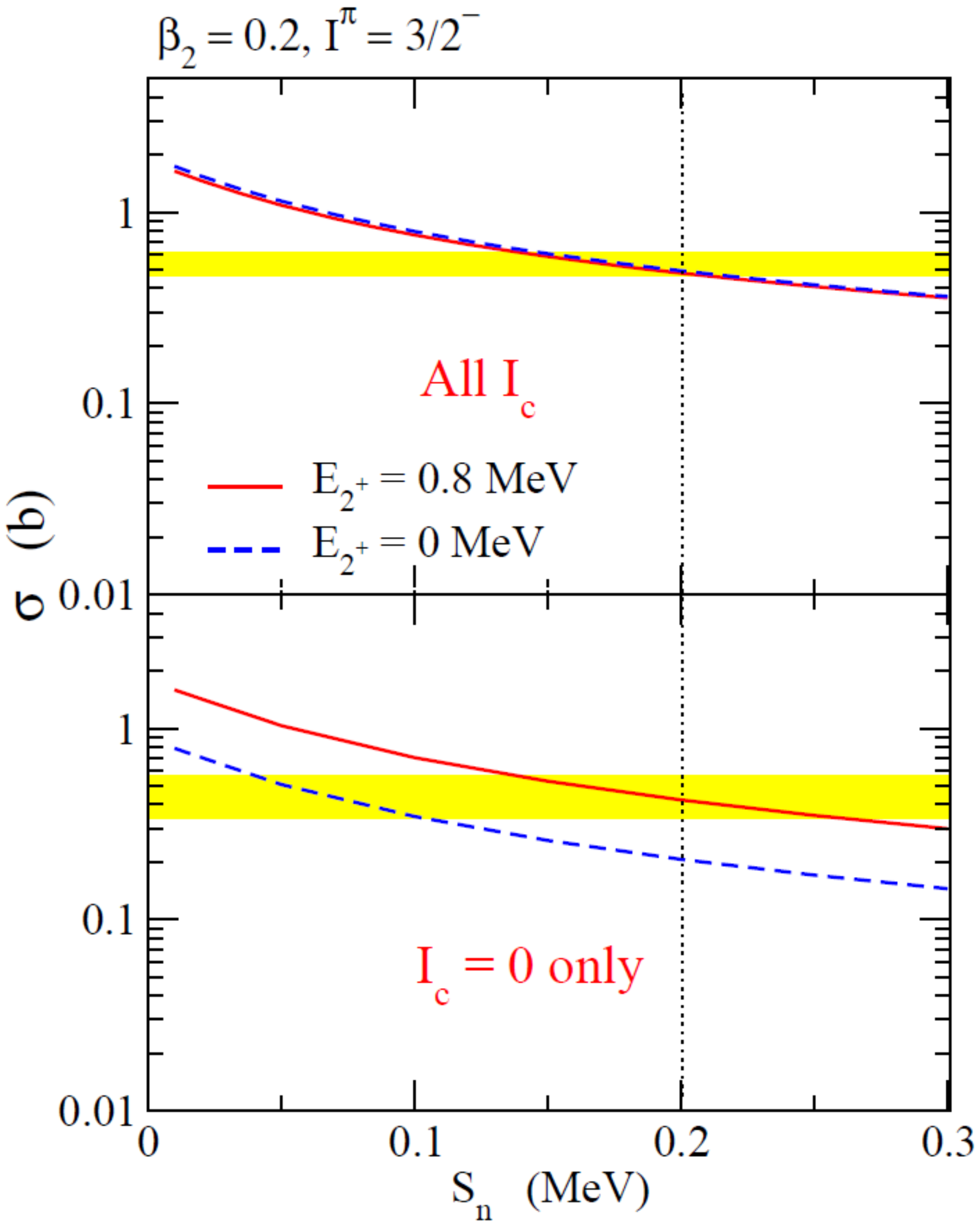

$^{31}Ne \rightarrow {}^{30}Ne\ (0^+) + n$

↑ Coul.BU

$\sigma_{bu}(0^+) = 0.45(11)$ b

T. Nakamura et al., preliminary data

cf. $\sigma_{bu}(\text{any } I_c) = 0.54(7)$ b

RPM for $S_n = 0.2$ MeV

$\sigma_{bu}(0^+) = 0.443$ b

good agreement with the data

cf. Nilsson: $\sigma_{bu}(0^+) = 0.216$ b

Coulomb breakup cross sections (β ~ 0.55 configuration)

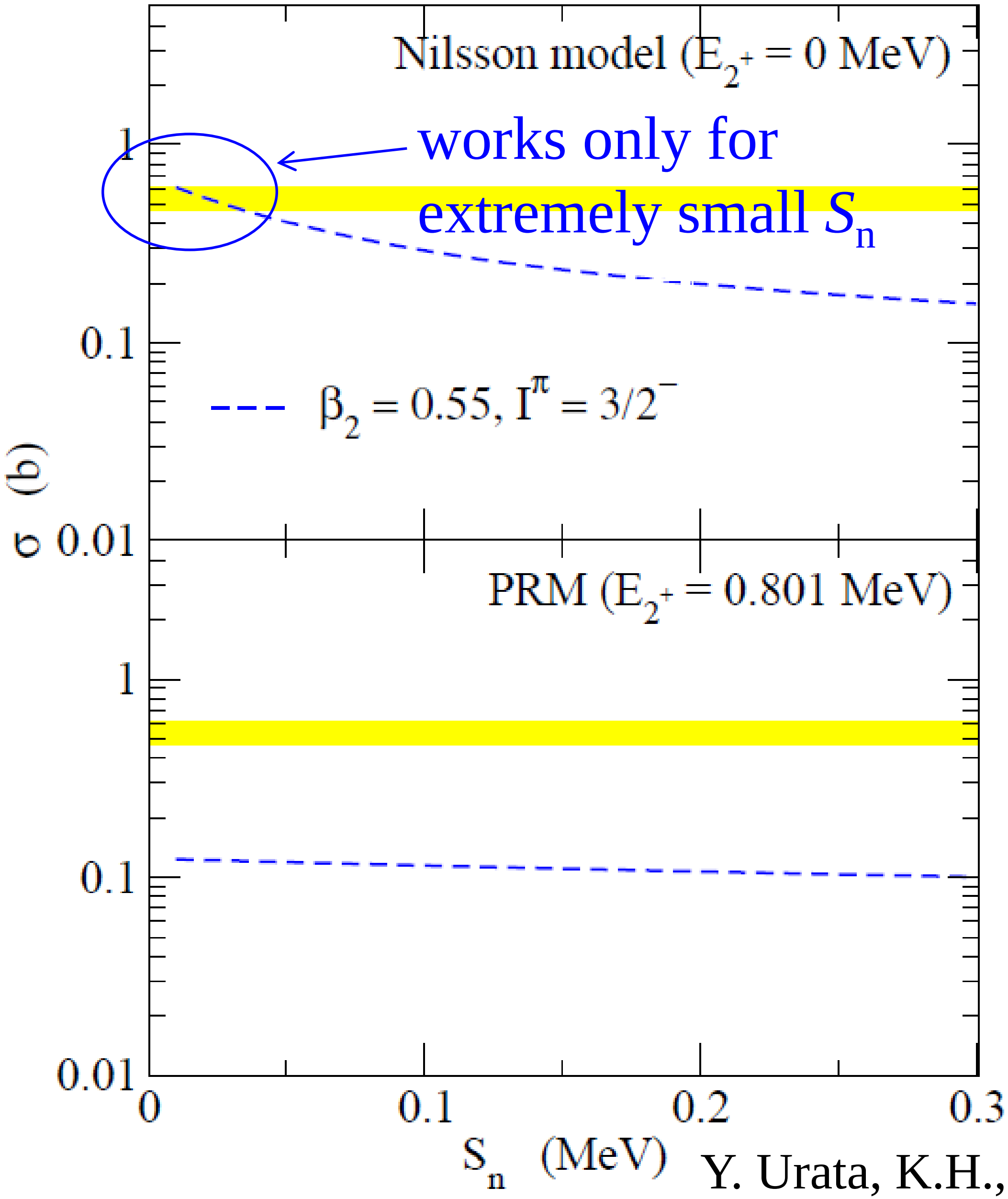

β ~ 0.55 : large non-adiabatic effects

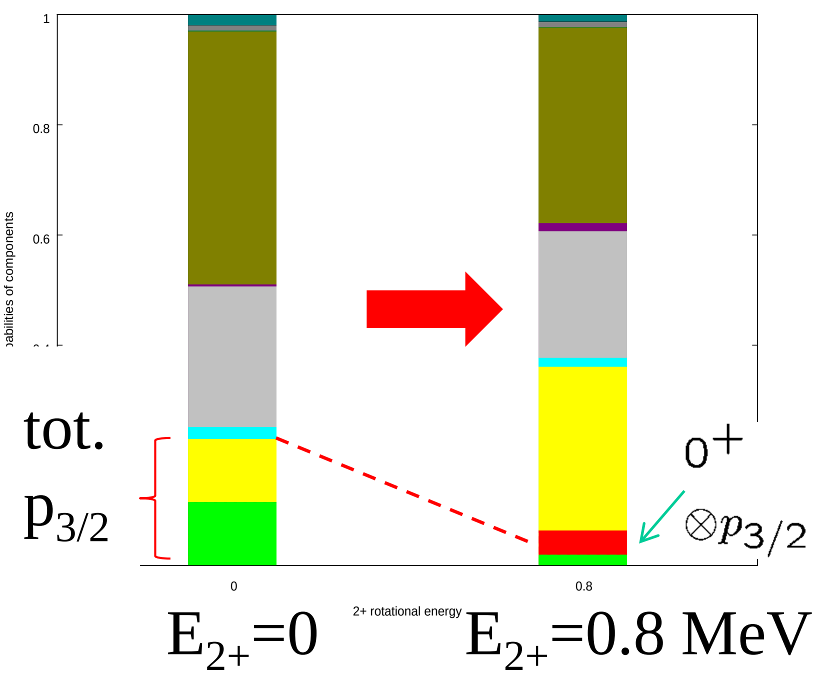

Y. Urata, K.H., and H. Sagawa, PRC83('11)041303(R)

Coulomb breakup cross sections ($\beta \sim 0.95$ configuration)

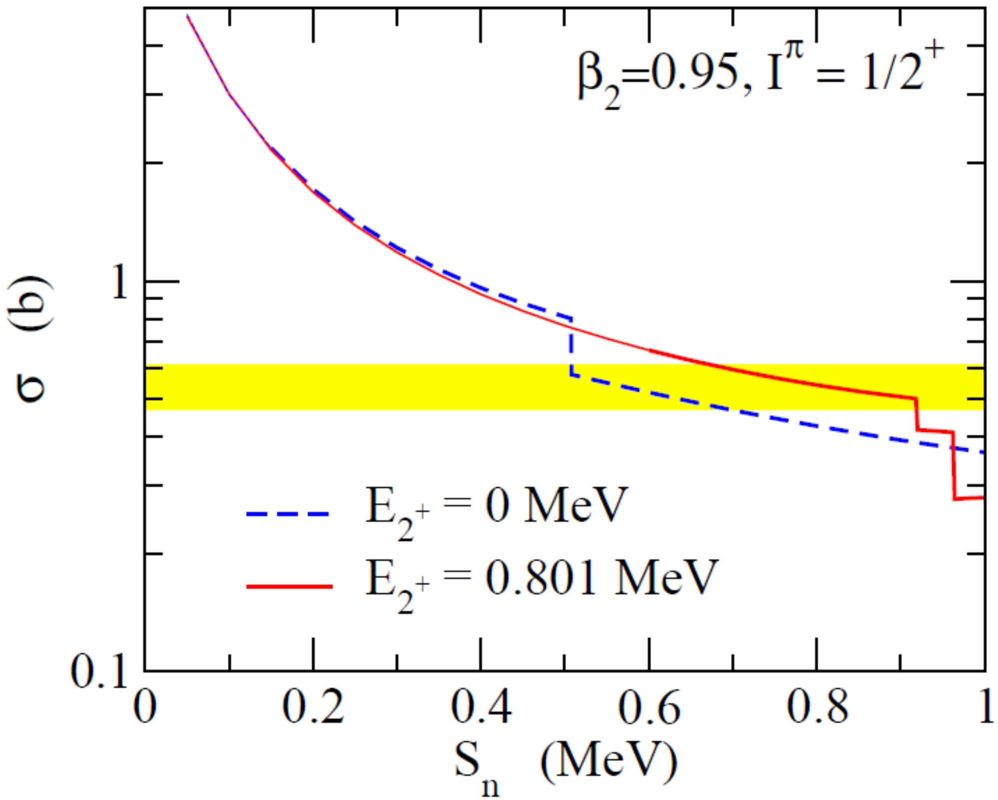

s-wave halo

$[0^+ \otimes s_{1/2}]$ ~ 80%

consistent with experimental σ only for $S_n \sim 0.8$ MeV

⟶ excluded by the recent new measurement for S_n

S_n = 0.29 +/- 1.64 MeV B. Jurado et al., PLB649 ('07) 43.

➡ S_n = -0.06 +/- 0.41 MeV L. Gaudefroy et al.,
PRL109('12) 202503

Reaction Cross section

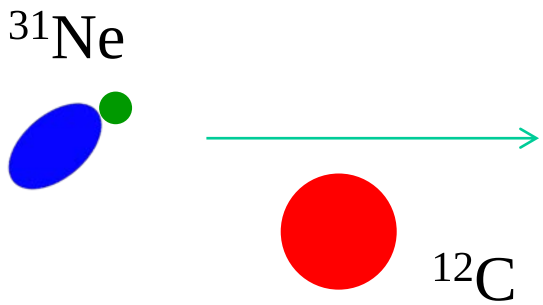

cf. P. Batham, I.J. Thompson, J.A. Tostevin, PRC71('05)064608:

Single-nucleon knockout reaction with particle-rotor model

- Few-body treatment for Glauber theory
- Zero-range approximation

extension to reaction cross sections

Y. Urata, K.H., H. Sagawa, PRC86('12)044613

$$\sigma_R = \int d\boldsymbol{b} \left(1 - \frac{1}{2I+1}\sum_M |\ \langle \Psi_{IM} \,|\, S_c S_v \,|\, \Psi_{IM}\rangle\ |^2\right)$$

$$S_c = \exp[-\bar{\sigma}_{\rm NN}(1 - i\bar{\alpha}_{\rm NN})\chi_c(\boldsymbol{b}_c, \hat{\boldsymbol{r}}_c)/2]$$

$$\chi_c(\boldsymbol{b}_c, \hat{\boldsymbol{r}}_c) = \int dz_c \int d\boldsymbol{r}' \rho_c(\boldsymbol{r}', \hat{\boldsymbol{r}}_c)\rho_T(|\boldsymbol{r}' + \boldsymbol{R}_c|)$$

^{30}Ne density ρ_c: Nilsson model, target density ρ_T: Gaussian

Reaction cross section

^{30,31}Ne + C (E/A = 240 MeV)

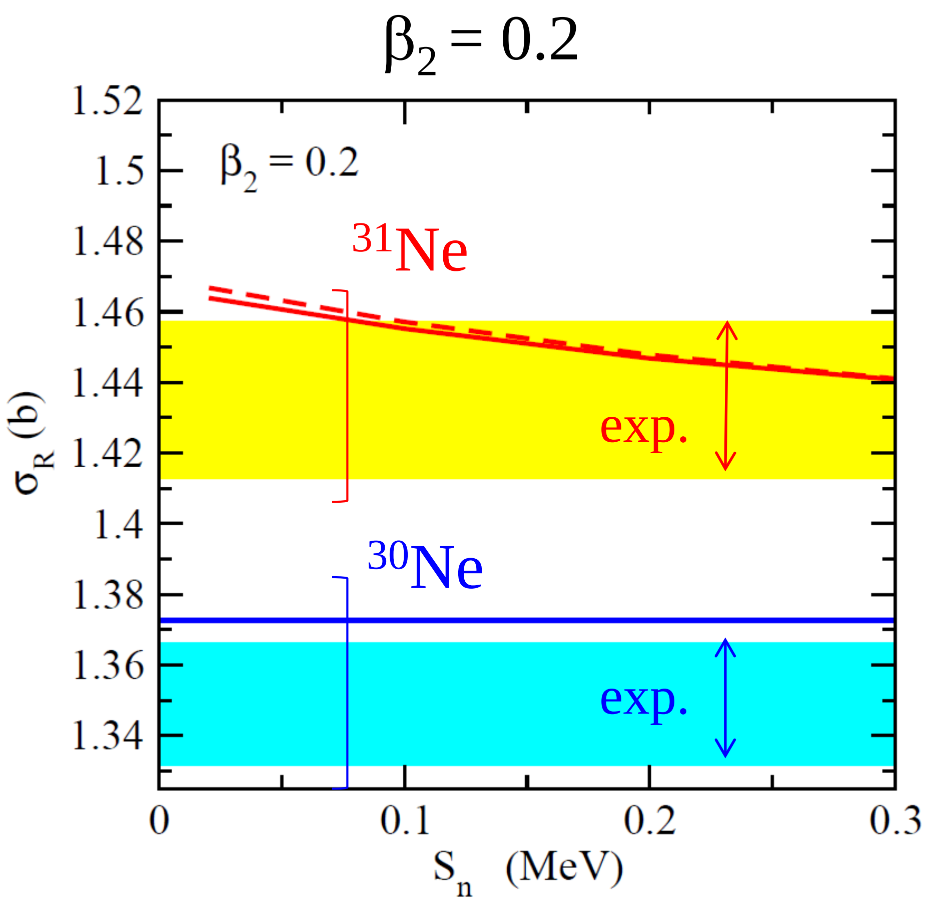

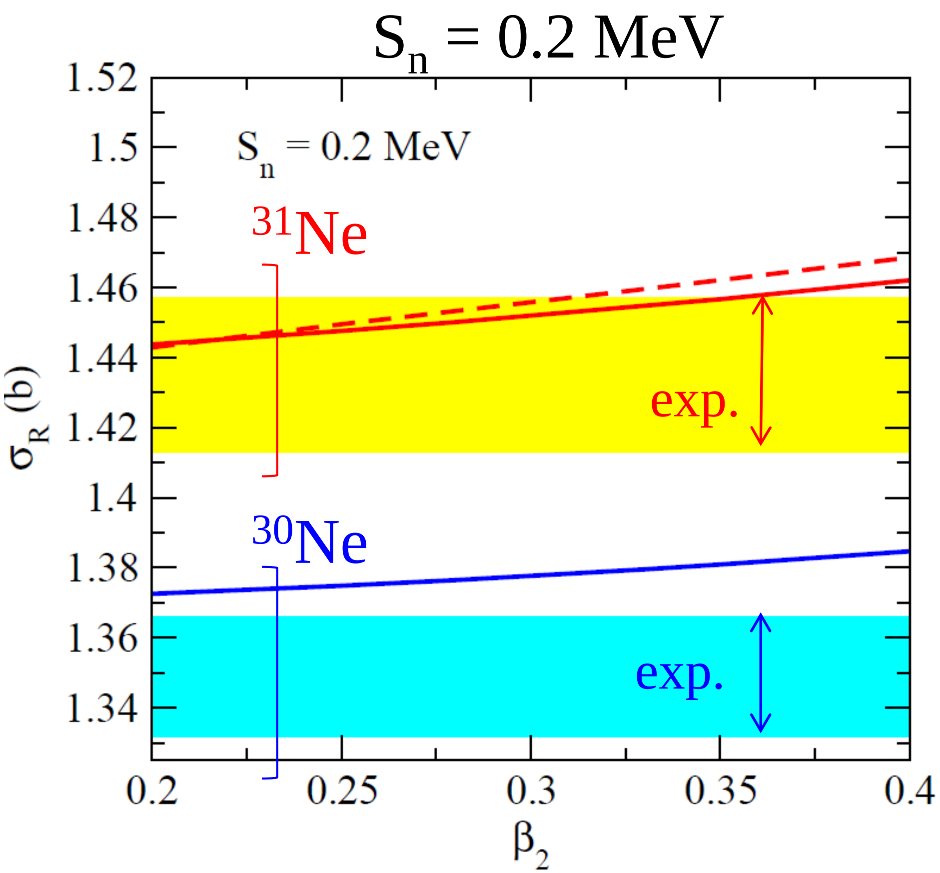

Y. Urata, K.H., and H. Sagawa,
PRC86('12)044613

Reaction cross section

^{30,31}Ne + C (E/A = 240 MeV)

$\beta_2 = 0.2$

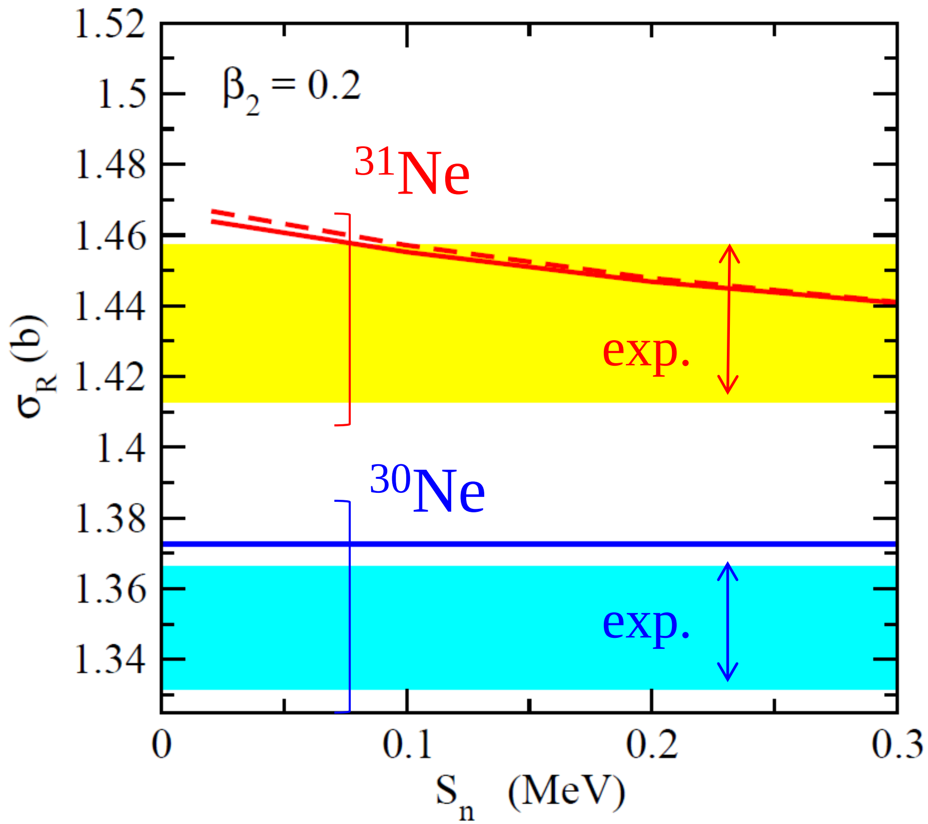

$S_n = 0.2$ MeV

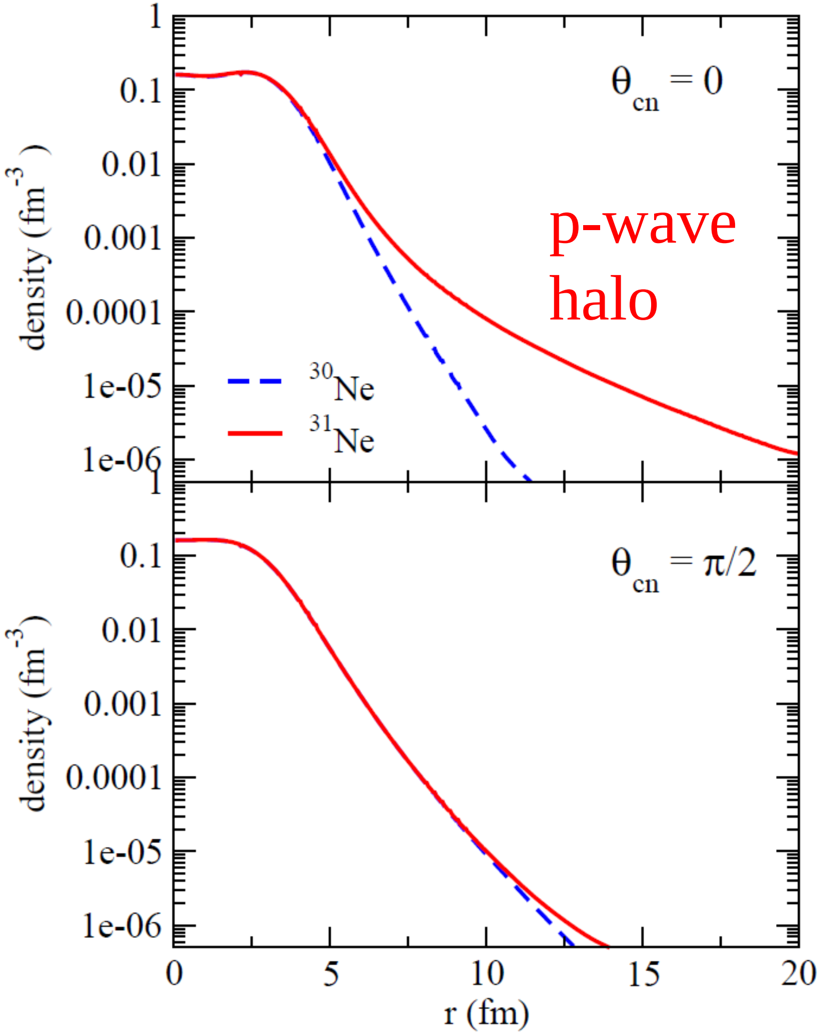

Y. Urata, K.H., and H. Sagawa,
PRC86('12)044613

Reaction cross section

^{30,31}Ne + C (E/A = 240 MeV)

$\beta_2 = 0.2$

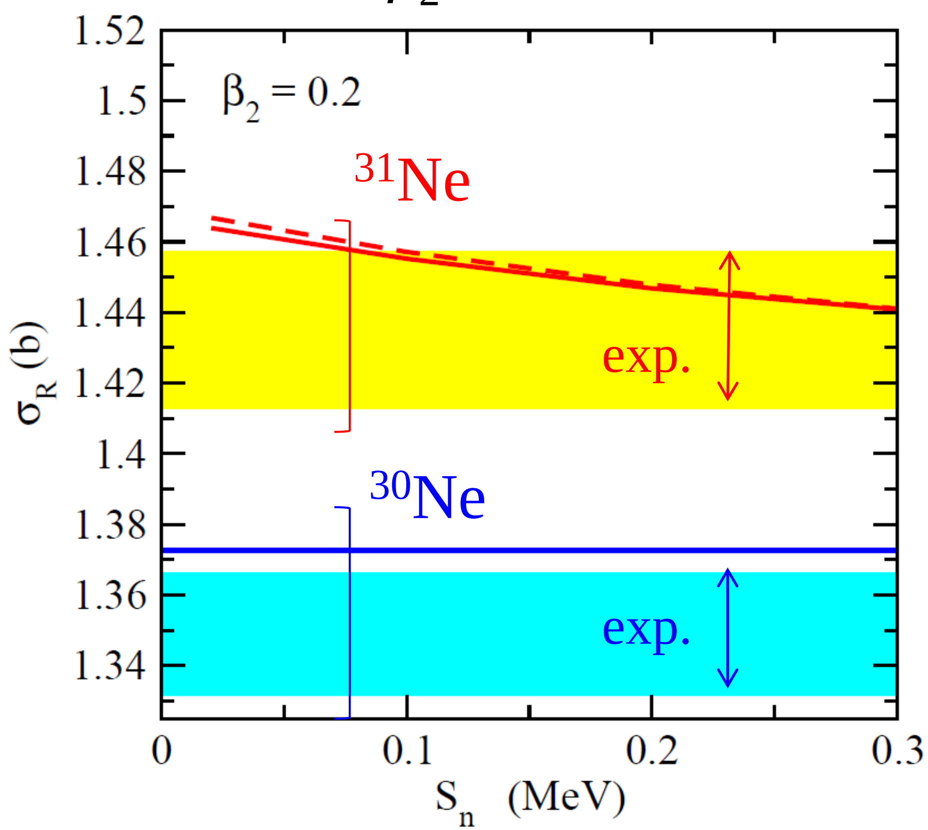

$I^\pi = 3/2^-$ at $\beta \sim 0.2$:
consistent both with $\sigma_{C\text{-}bu}$ and σ_R

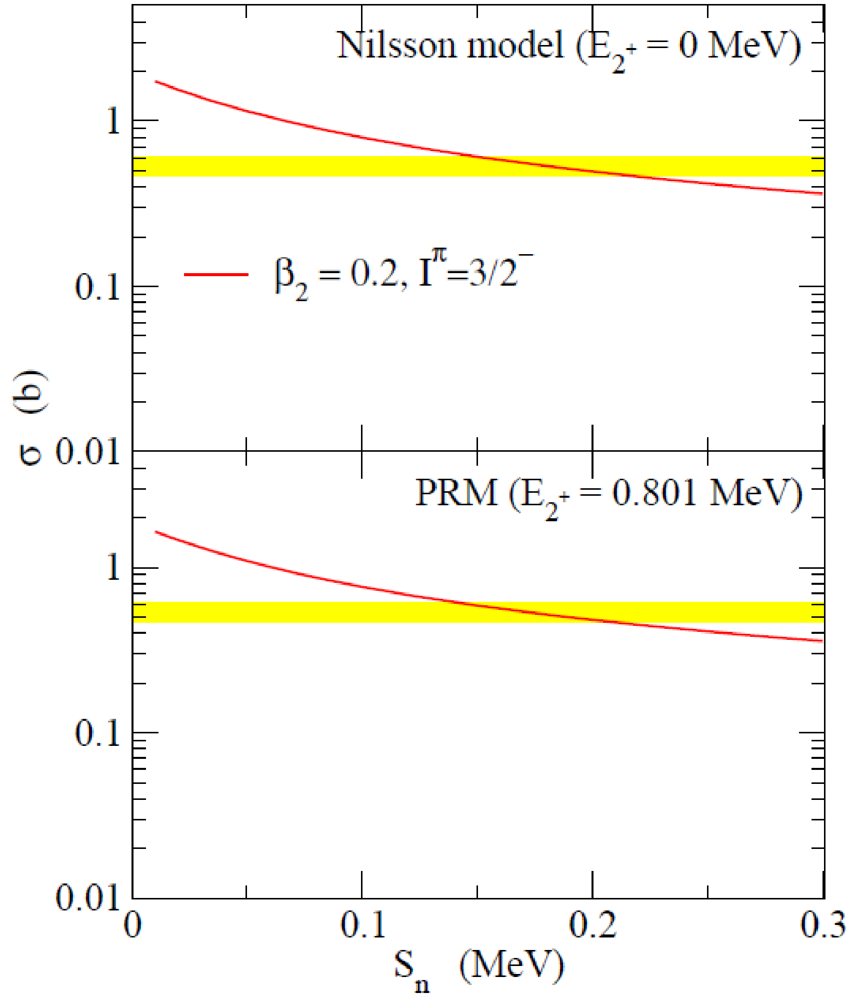

Y. Urata, K.H., and H. Sagawa,
PRC86(‘12)044613

1n removal cross section

$$\sigma_{-1n}(^{31}\mathrm{Ne}) \sim \sigma_R(^{31}\mathrm{Ne}) - \sigma_R(^{30}\mathrm{Ne})$$

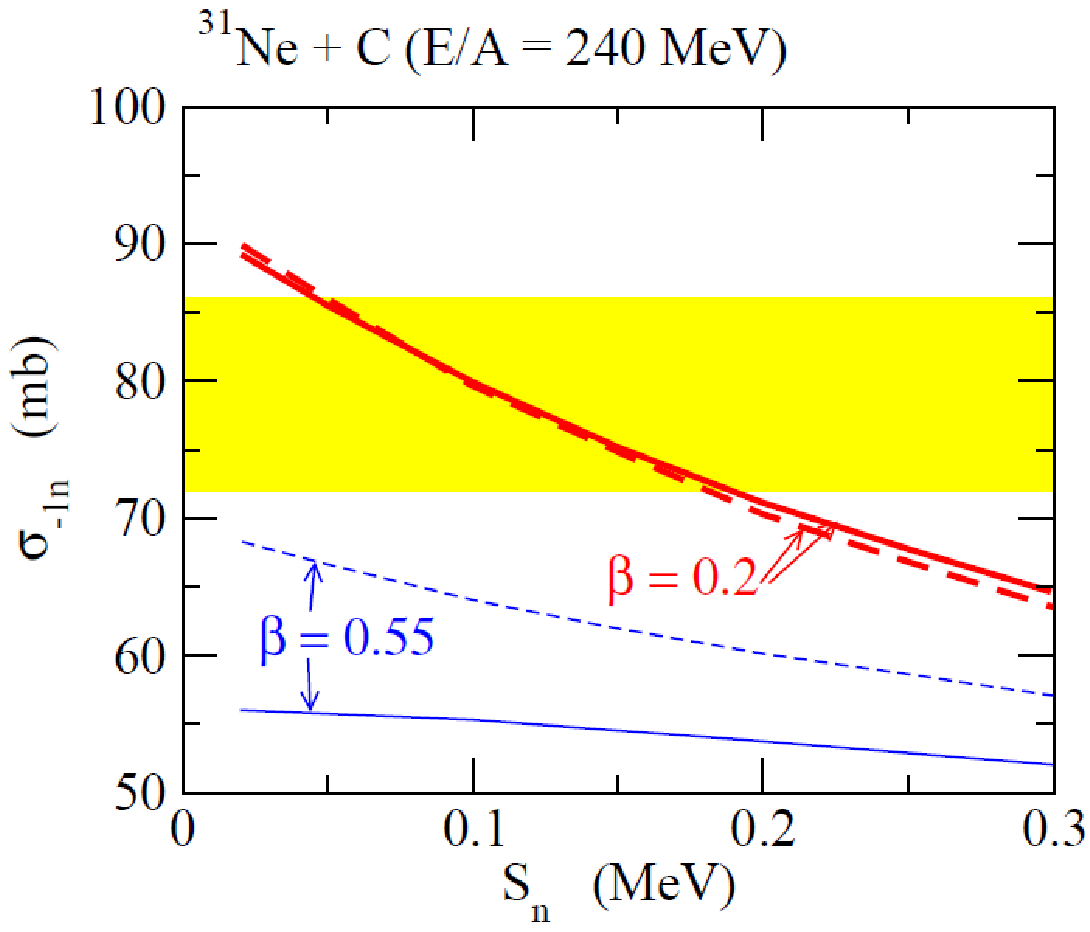

Y. Urata, K.H., and H. Sagawa,
PRC86('12)044613

Odd-even staggering of interaction cross sections

σ_I of unstable nuclei: often show a large odd-even staggering

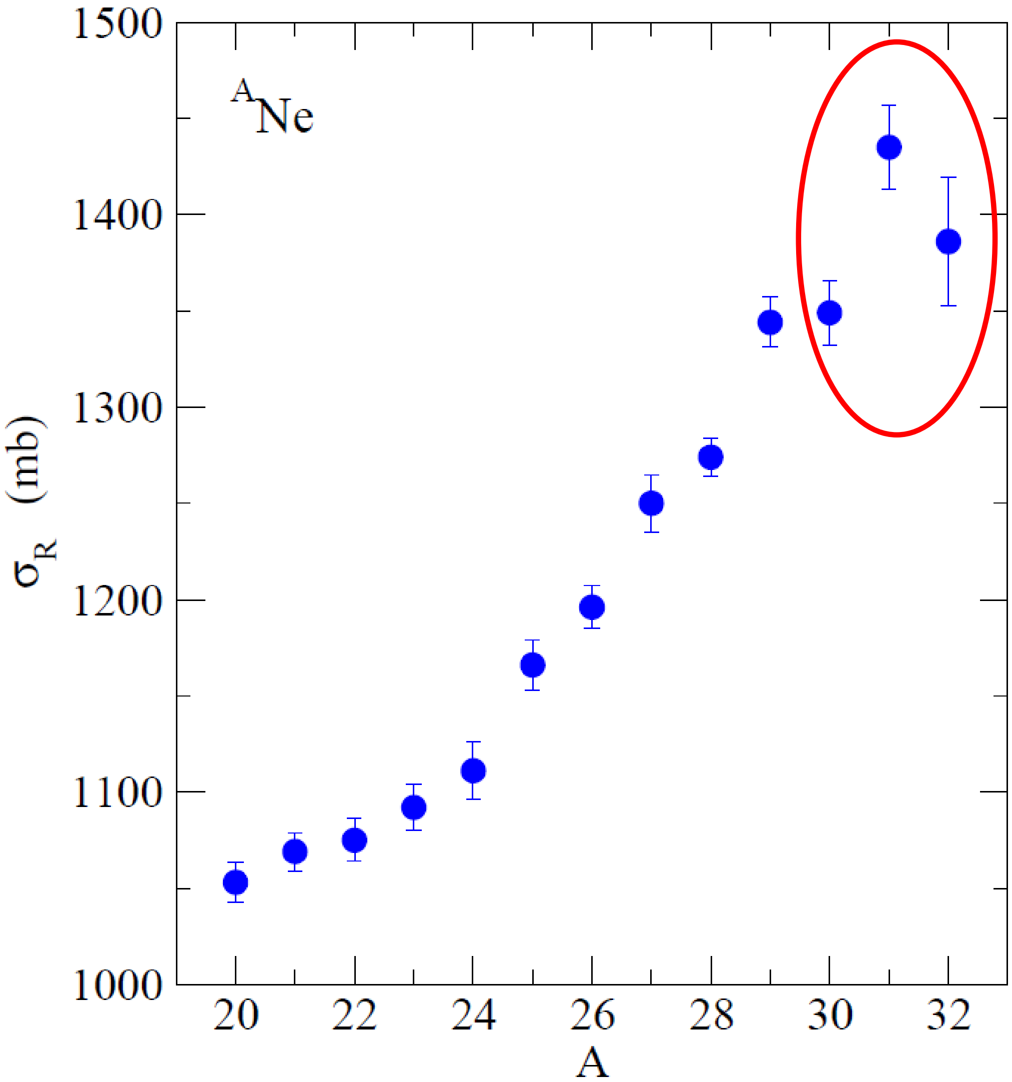

Typical example:

Recent experimental data on Ne isotopes

M. Takechi et al., Phys. Lett. B707 ('12) 357

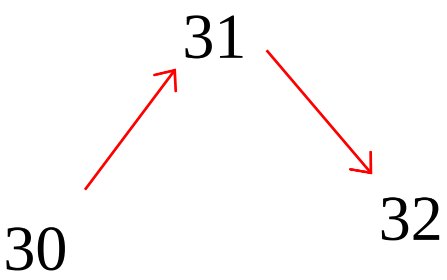

clear odd-even effect

- deformation effect?
- pairing effect?

Systematics

OES parameter

$$\gamma_3 \equiv -\frac{1}{2}[\sigma_R(A+2) - 2\sigma_R(A+1) + \sigma_R(A)]$$

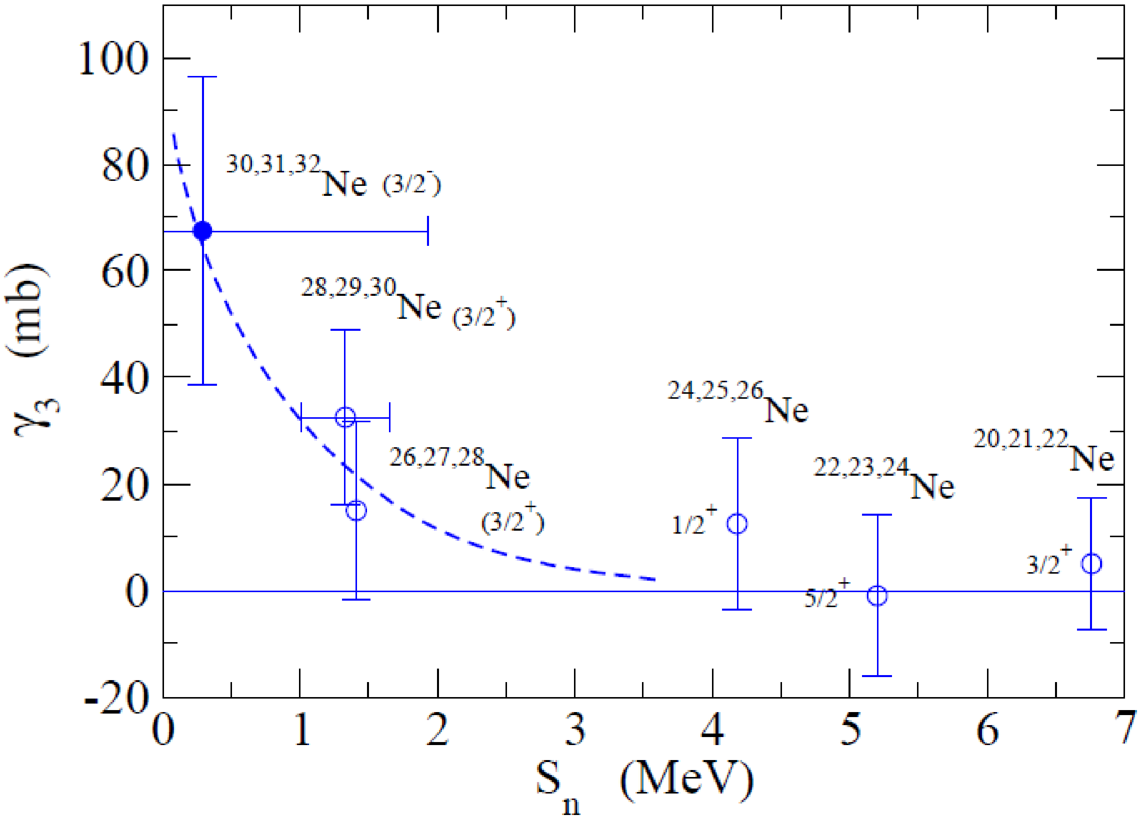

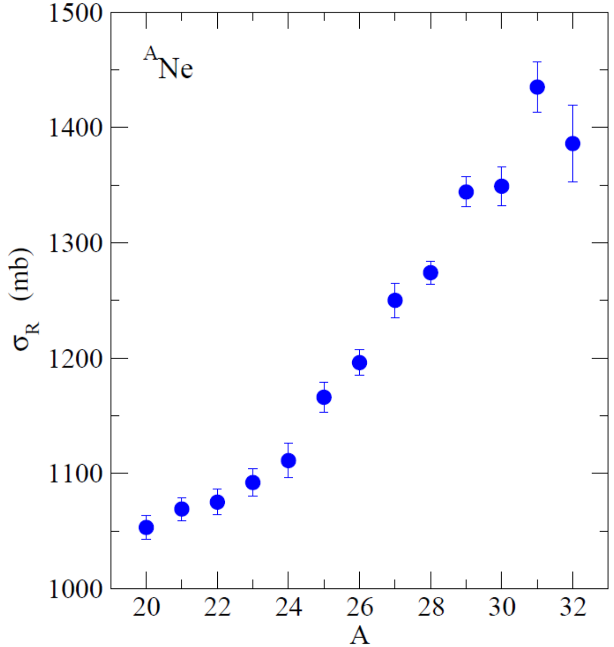

K. H. and H. Sagawa, PRC85('12)014303

rms radius and reaction cross section

HFB with a spherical Woods-Saxon

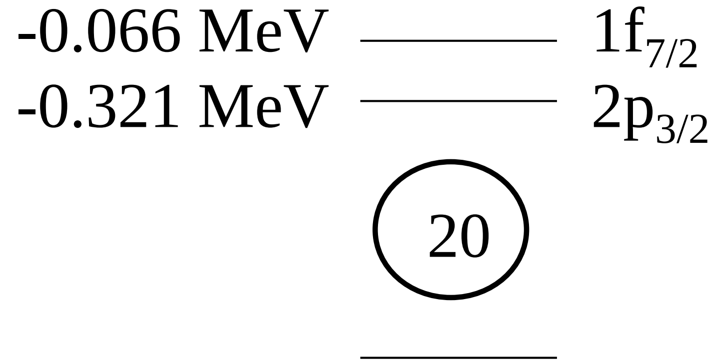

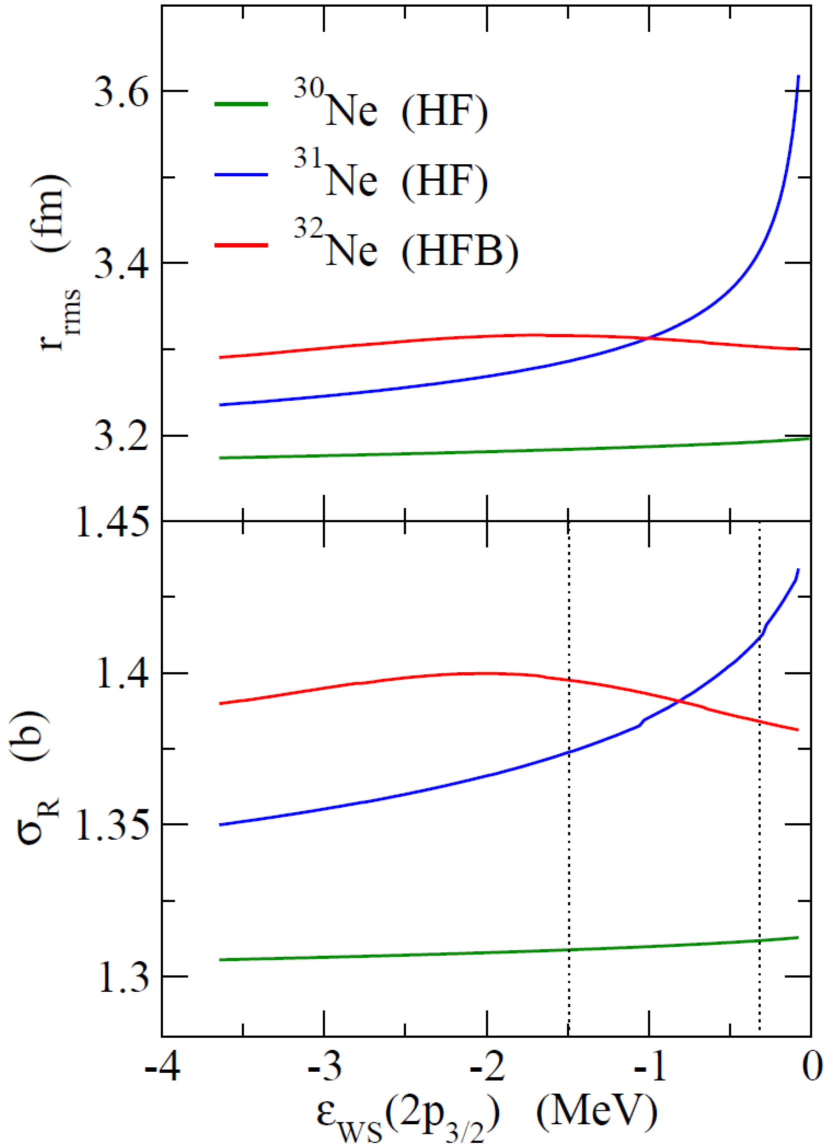

^{31}Ne (a =0.75 fm)

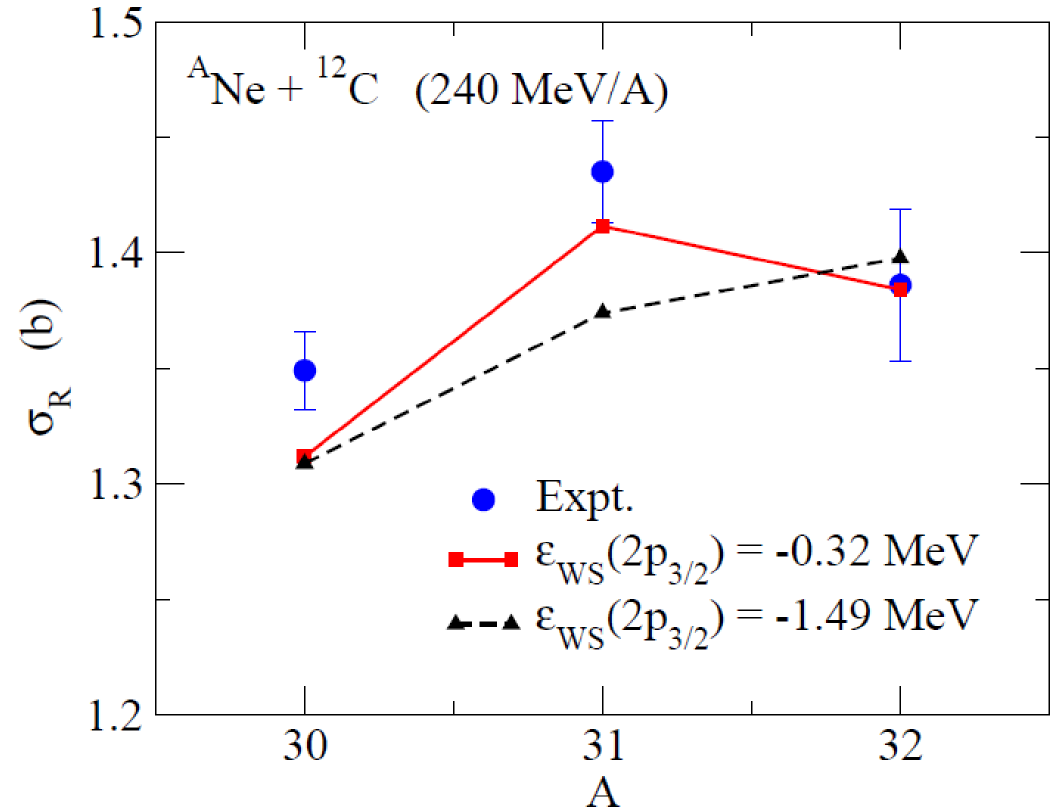

K. H. and H. Sagawa, PRC84('11)011303(R)

Systematics

OES parameter

$$\gamma_3 \equiv -\frac{1}{2}[\sigma_R(A+2) - 2\sigma_R(A+1) + \sigma_R(A)]$$

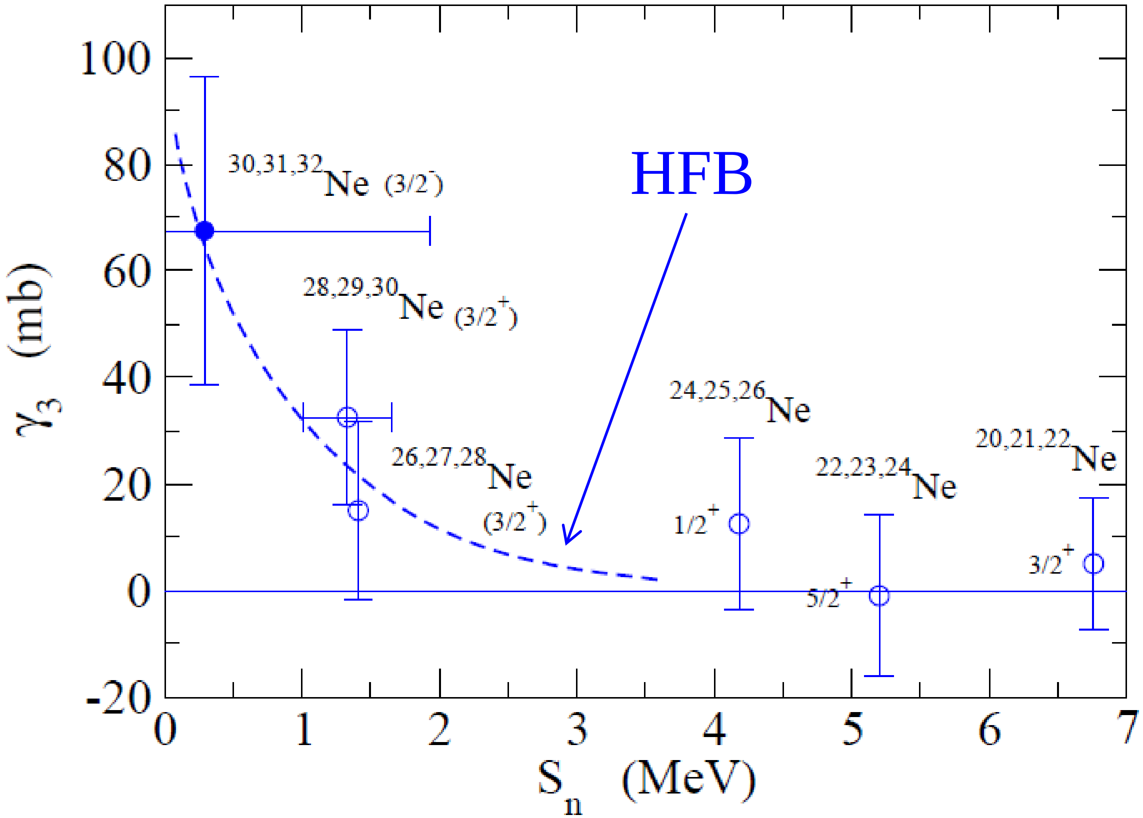

K. H. and H. Sagawa, PRC85('12)014303

Summary and Discussions

deformation $\longrightarrow$ mixture of angular momenta

$\longrightarrow$ enlarges a possibility of halo formation

- good example: ^{31}Ne

$0^+ \times p_{3/2}$: 44.9 %
$2^+ \times p_{3/2}$: 8.4 %
$2^+ \times f_{7/2}$: 42.7 %

$\longleftarrow$ non-adiabatic particle-rotor model with $\beta \sim 0.2$

➡ well accounts for $\sigma_{C\text{-}bu}$ (tot), $\sigma_{C\text{-}bu}(0^+)$, and σ_R simultaneously

- Odd-even staggering of σ_R

✓an important role of pairing correlation
✓OES parameter: a good tool to investigate the pairing correlation
✓role of deformation? $\longleftarrow$ deformed HFB (a work in progress)

Perspectives: deformed (halo) nuclei

✓"Fine structure" in breakup/transfer reactions

direct population of the 2^+ state after breakup/transfer

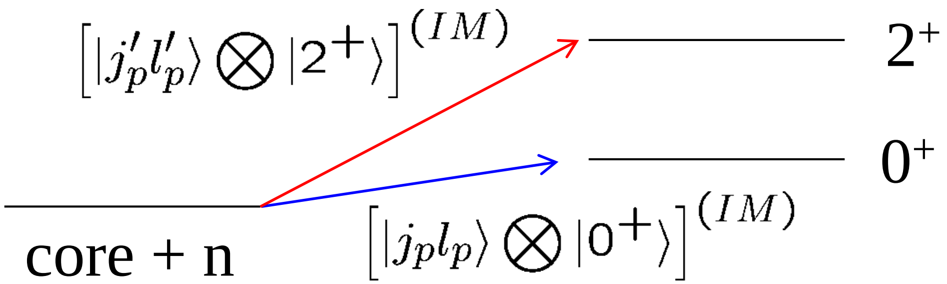

cf. proton decay

cf. Nakamura-san's expt.

detection of 2α from ^{9}Be+^{209}Bi

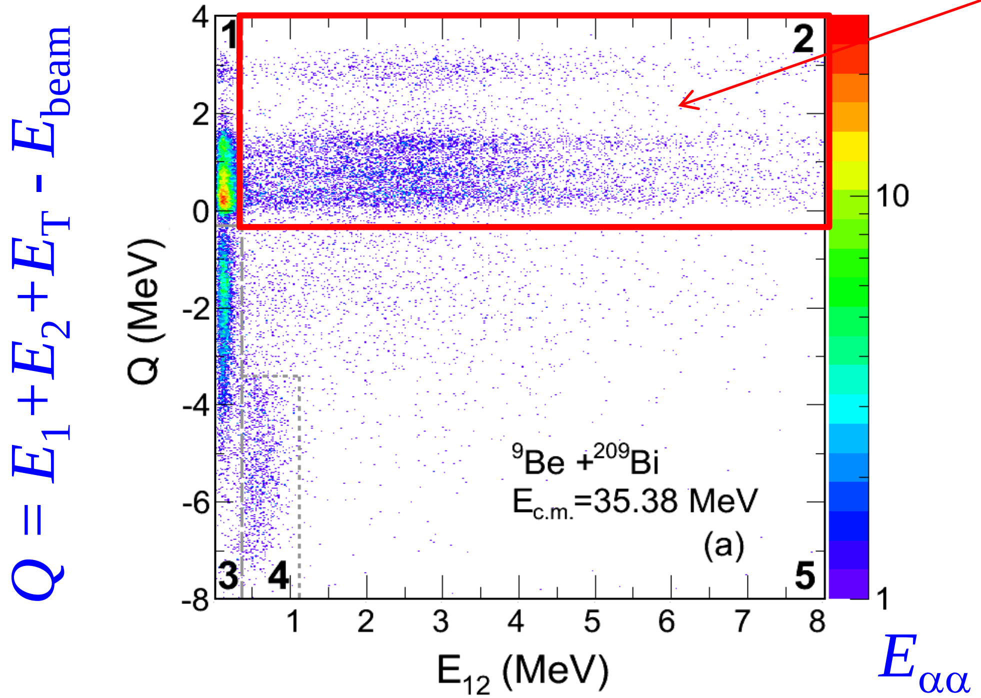

^{209}Bi(^{9}Be,^{8}Be*)^{210}Bi

- **direct population of ^{8}Be* (2^+ and 4^+)**
- prompt breakup
- relevant to incomplete fusion

cf. Q_{gg} = + 2.94 MeV for ^{209}Bi(^{9}Be,^{8}Be)^{210}Bi

R. Rafiei et al., PRC81('10)024601